NATIONAL ADVISORY COMMITTEE FOR AERONAUTICS

REPORT No. 394

AIRSHIP MODEL TESTS IN THE VARIABLE DENSITY WIND TUNNEL

By IRA H. ABBOTT

1931

For sale by the Superintendent of Documents, Washington, D. C. . . . . Price 20 cents

AERONAUTICAL SYMBOLS

1. FUNDAMENTAL AND DERIVED UNITS

	Symbol	Metric		English	
		Unit	Symbol	Unit	Symbol
Length	l	meter	m	foot (or mile)	ft. (or mi.)
Time	t	second	s	second (or hour)	sec. (or hr.)
Force	F	weight of one kilogram	kg	weight of one pound	lb.
Power	P	kg/m/s		horsepower	hp
Speed		km/h	k. p. h.	mi./hr.	m. p. h.
		m/s	m. p. s.	ft./sec.	f. p. s.

2. GENERAL SYMBOLS, ETC.

W, Weight $= mg$

g, Standard acceleration of gravity $= 9.80665$ m/s^2 $= 32.1740$ ft./sec.^{2}

m, Mass $= \frac{W}{g}$

ρ, Density (mass per unit volume).

Standard density of dry air, 0.12497 (kg-m^{-4} s^2) at 15° C. and 750 mm $= 0.002378$ (lb.-ft.$^{-4}$ sec.^{2}).

Specific weight of "standard" air, 1.2255 kg/m^3 $= 0.07651$ lb./ft.^{3}.

mk^2, Moment of inertia (indicate axis of the radius of gyration k, by proper subscript).

S, Area.

S_w, Wing area, etc.

G, Gap.

b, Span.

c, Chord.

$\frac{b^2}{S}$, Aspect ratio.

μ, Coefficient of viscosity.

3. AERODYNAMICAL SYMBOLS

V, True air speed.

q, Dynamic (or impact) pressure $= \frac{1}{2}\rho V^2$.

L, Lift, absolute coefficient $C_L = \frac{L}{qS}$

D, Drag, absolute coefficient $C_D = \frac{D}{qS}$

D_o, Profile drag, absolute coefficient $C_{D_o} = \frac{D_o}{qS}$

D_i, Induced drag, absolute coefficient $C_{D_i} = \frac{D_i}{qS}$

D_p, Parasite drag, absolute coefficient $C_{D_p} = \frac{D_p}{qS}$

C, Cross-wind force, absolute coefficient $C_C = \frac{C}{qS}$

R, Resultant force.

i_w, Angle of setting of wings (relative to thrust line).

i_t, Angle of stabilizer setting (relative to thrust line).

Q, Resultant moment.

Ω, Resultant angular velocity.

$\rho\frac{Vl}{\mu}$, Reynolds Number, where l is a linear dimension.

e. g., for a model airfoil 3 in. chord, 100 mi./hr. normal pressure, at 15° C., the corresponding number is 234,000;

or for a model of 10 cm chord 40 m/s, the corresponding number is 274,000.

C_p, Center of pressure coefficient (ratio of distance of $c.\ p.$ from leading edge to chord length).

α, Angle of attack.

ϵ, Angle of downwash.

α_o, Angle of attack, infinite aspect ratio.

α_i, Angle of attack, induced.

α_a, Angle of attack, absolute.

(Measured from zero lift position.)

γ, Flight path angle.

REPORT No. 394

AIRSHIP MODEL TESTS IN THE VARIABLE DENSITY WIND TUNNEL

By IRA H. ABBOTT
Langley Memorial Aeronautical Laboratory

58997—31——1

NATIONAL ADVISORY COMMITTEE FOR AERONAUTICS

NAVY BUILDING, WASHINGTON, D. C.

(An independent Government establishment, created by act of Congress approved March 3, 1915, for the supervision and direction of the scientific study of the problems of flight. Its membership was increased to 15 by act approved March 2, 1929 (Public, No. 908, 70th Congress). It consists of members who are appointed by the President, all of whom serve as such without compensation.)

EXECUTIVE COMMITTEE

REPORT No. 394

AIRSHIP MODEL TESTS IN THE VARIABLE DENSITY WIND TUNNEL

By Ira H. Abbott

SUMMARY

An investigation of the aerodynamic characteristics of airship models was made in the variable density wind tunnel of the National Advisory Committee for Aeronautics. Eight Goodyear-Zeppelin airship models, supplied by the Bureau of Aeronautics of the Navy Department, were tested in the original closed-throat tunnel. After the tunnel was rebuilt with an open throat a new model was tested, and one of the Goodyear-Zeppelin models was retested. These tests were made at tank pressures varying from 1 to 20 atmospheres, and the extreme range of Reynolds Number was about 1,000,000 to 40,000,000. The lift, drag, and moment coefficients of the models were determined, and the effects upon these coefficients of pitch, fineness ratio, scale, surface texture, initial degree of air-stream turbulence, and the effects of the addition of fins and cars were investigated. The resulting curves are included.

The results show that the addition of fins and car to the bare hull of a model causes an increase in lift at positive angles of pitch and causes an additional drag which increases with the pitch. Little change in drag coefficient was found between a fineness ratio of about five and seven. The effect of surface roughness on drag was found to be very large. The drag coefficient and the apparent effect of scale depend upon the initial degree of air-stream turbulence. The results indicate that much may be done to determine the drag of airships from evaluations of the pressure and skin-frictional drags on models tested at large Reynolds Numbers.

INTRODUCTION

Wind-tunnel tests of airship models have resulted in many useful data on the aerodynamic characteristics of airship hulls, and on the effects of fineness ratio, fins and control surfaces, and protuberances. These data have been useful in airship design, but their usefulness has been limited greatly by the fact that the Reynolds Numbers of the tests are very small as compared to those obtained in flight. This limitation is especially evident from a consideration of the drag coefficient which shows a more pronounced variation with Reynolds Number than do the other characteristics.

Not only does the drag coefficient obtained from a model apparently have little relation to the full-scale coefficient, but also the drag coefficient of the same model as obtained in different tunnels at the same value of the Reynolds Number varies greatly. Consequently, the results of wind-tunnel tests on airship models have been generally discredited, and airship design has been hampered by the impossibility of predicting the drags of proposed airships from model tests. Work done in the past few years has indicated the possibility of clarifying the problem by the application of Prandtl's boundary-layer theory, but so few tests have been made over a large range of Reynolds Numbers that little experimental data have been available to show that the application of this theory is possible to a reasonable extent.

An investigation of the aerodynamic characteristics of airship models was conducted over a large range of Reynolds Numbers in the variable density wind tunnel of the National Advisory Committee for Aeronautics. Some of the tests were made in the original closed-throat tunnel, and the remainder were made in the tunnel as rebuilt with an open throat. This arrangement made it possible to compare the results of tests made over a large range of Reynolds Numbers in two tunnels.

The tests included the determination of lift, drag, and moment coefficients of eight Goodyear-Zeppelin airship models, and of a model of the ZRS–4 airship. Each model was tested with and without appendages, and one model was tested with three degrees of surface roughness. The models were supplied by the Bureau of Aeronautics of the Navy Department.

The drags of the models were measured at zero pitch with the models mounted on two types of suspension to allow the corrections made for support drag and interference to be checked. Corrections were made for the effect of air-stream convergence on the drag, and they were checked by testing one model in tunnel positions corresponding to different static pressure gradients.

Curves of lift, drag, and moment coefficients are given for nine models. Other curves show the effects of pitch, fineness ratio, appendages, surface texture, and scale.

APPARATUS

Eight Goodyear-Zeppelin airship models and one model of the ZRS–4 airship were tested in this investigation. All the models were made of mahogany with metal nose and tail caps, and the cross sections were 24-sided polygons, fairing to circles at the nose and to 16-sided polygons at the tail. The fineness ratio of the ZRS–4 model was 5.9. The Goodyear-Zeppelin series consisted of four basic models with fineness ratios of 3.6, 4.8, 6.0, and 7.2, having the same maximum diameter, but varying in length. Four additional models with fineness ratios of 5.3, 5.6, 5.8, and 6.8 were obtained by inserting parallel middle bodies in the two smallest basic models. Figure 1 illustrates the models and the means used to lengthen the smaller ones. The middle bodies had a constant diameter equal to the maximum of the models, and their lengths were multiples of the diameter. All the Goodyear-Zeppelin models had the same generating curve, the ordinates of which are given in Table I. The ordinates of the ZRS–4 model are given in Table II. The center of buoyancy positions and volumes for all models are given in Table III. The models were equipped with removable fins and cars. Brass fins were fitted to the GZ–3.6 and the GZ–7.2 models, and wooden fins to all others. (Fig. 2.)

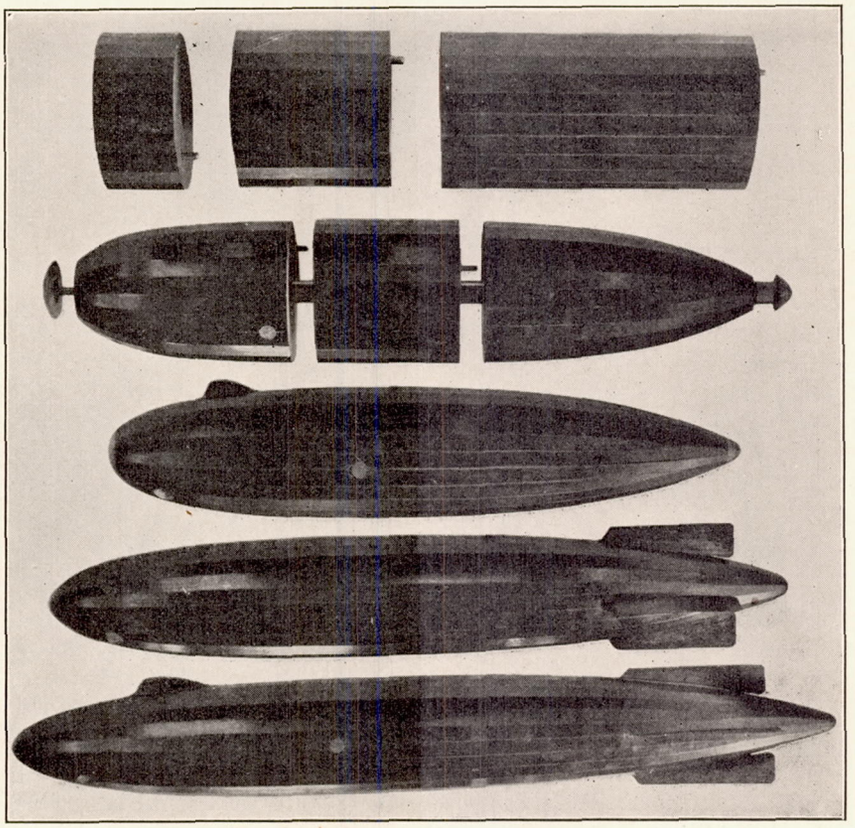

FIGURE 1.—Goodyear-Zeppelin airship models

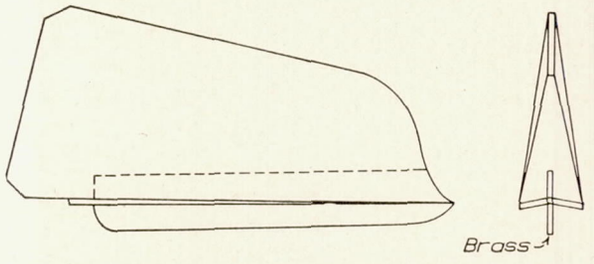

FIGURE 2.—Goodyear-Zeppelin airship models. Wood V fins. The brass fins are made of brass plate. They are of the same general plan form as the wood V fins and are 1/32 inch thick

All models had rubbed varnish finishes. One model was also tested with a highly polished surface, and with a surface coated with No. 180 carborundum (grains ranging from about 0.003 to 0.007 inch in maximum dimension). The granular carborundum was sprayed over the freshly varnished surface by means of a small air jet to obtain a uniform distribution.

A description of the original close-throat variable density wind tunnel and a discussion of the principles of its operation are given in reference 1. Aside from the change to an open throat, the rebuilt tunnel was much like the original, the chief differences being in the shape of the air passages and in the balance details. (Fig. 3.) Sphere drag tests (reference 2) showed that the open-throat tunnel had less air-stream turbulence than the old closed-throat tunnel.

Figures 4 and 5 show the method of mounting the models on the main balance in the original tunnel. Special supports were used with the outer ends fastened

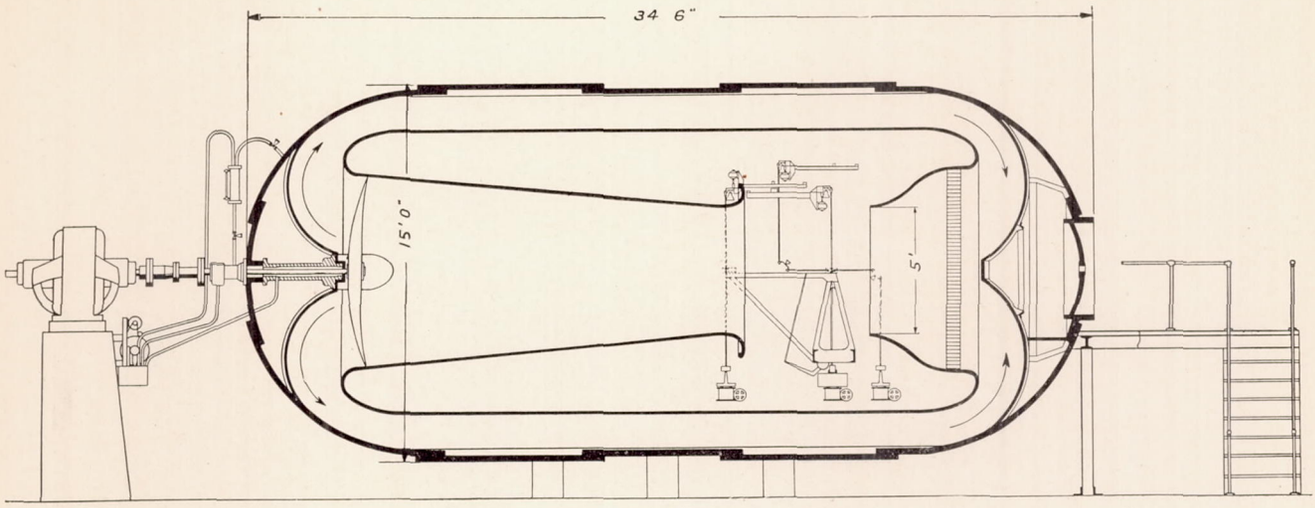

FIGURE 3.—Open-throat variable density wind tunnel

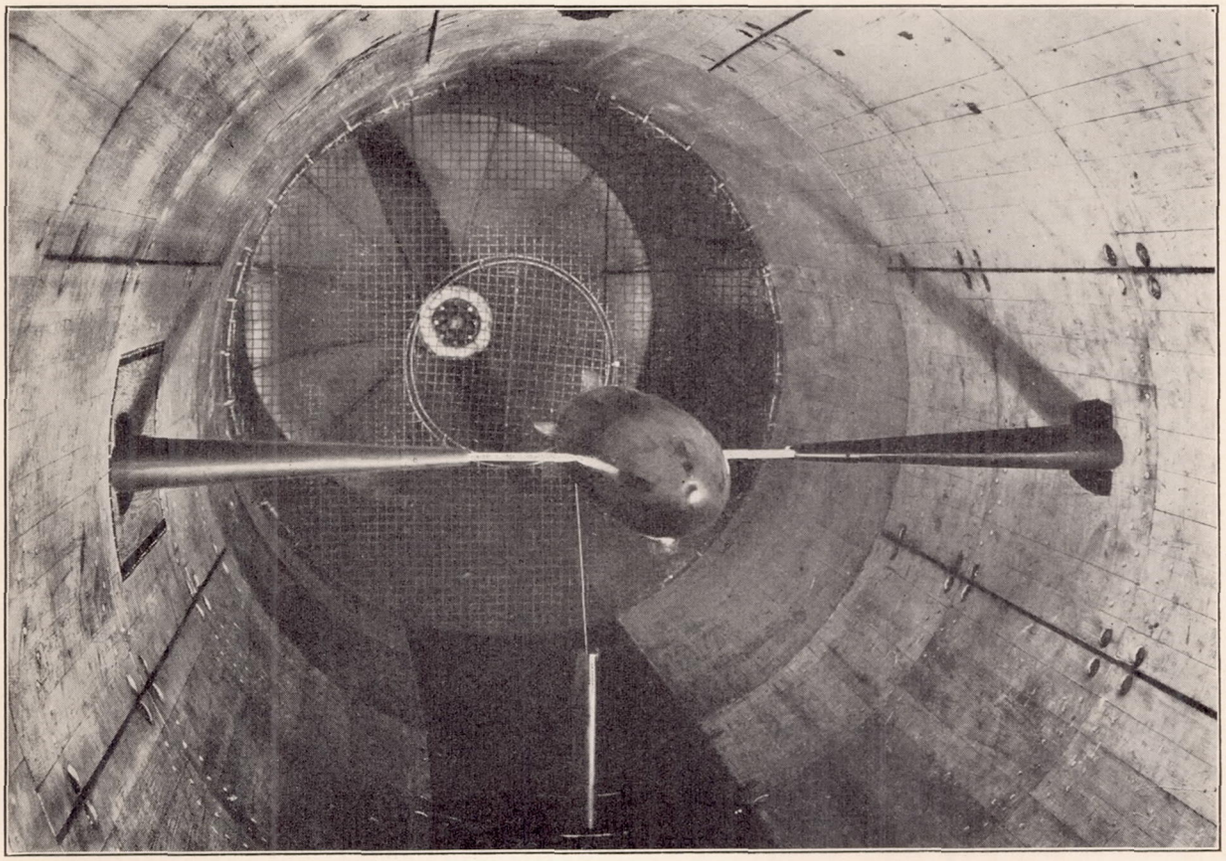

FIGURE 4.—Goodyear-Zeppelin airship model mounted at zero pitch on the main balance of the closed-throat tunnel

to the balance ring, and the others extended into a brass bushing in the model. This bushing formed the bearing around which the model pivoted with changing pitch. A streamline wire attached to the shielded, angle-of-pitch bar supported the tail of the model. Streamlined shields covered the supports.

The models were mounted on the main balance in the open-throat tunnel as shown in Figure 6. The main supports were fastened to the balance cradle at the bottom of the test chamber and were partly shielded. The exposed portions were streamlined. The models, which were mounted on a horizontal streamlined rod between the supports, contained brass bushings to form the bearings on which they pivoted with changing pitch. A partly shielded, streamline wire fastened to the angle-of-pitch bar formed the tail support.

A photograph of a model mounted on the auxiliary balance in the old, closed-throat tunnel is shown in Figure 7. This balance and mounting are fully described in reference 3. The mounting in the open-throat tunnel was the same, except that four round unshielded wires were used to support the model instead of three partly shielded streamline wires, and that a 45° linkage was used instead of a bell crank to transmit the force of a counterweight. (Fig. 8.)

METHOD

The tests were made in the usual manner in the variable density wind tunnel. (Reference 1.) The resultant force on the balance included the following:

1. The desired aerodynamic forces on the model.
2. Forces on the model due to air-stream convergence.
3. Forces on supports of model.
4. Forces due to mutual interference of model and supports.
5. Forces due to windage on parts of the balance located outside the air stream.

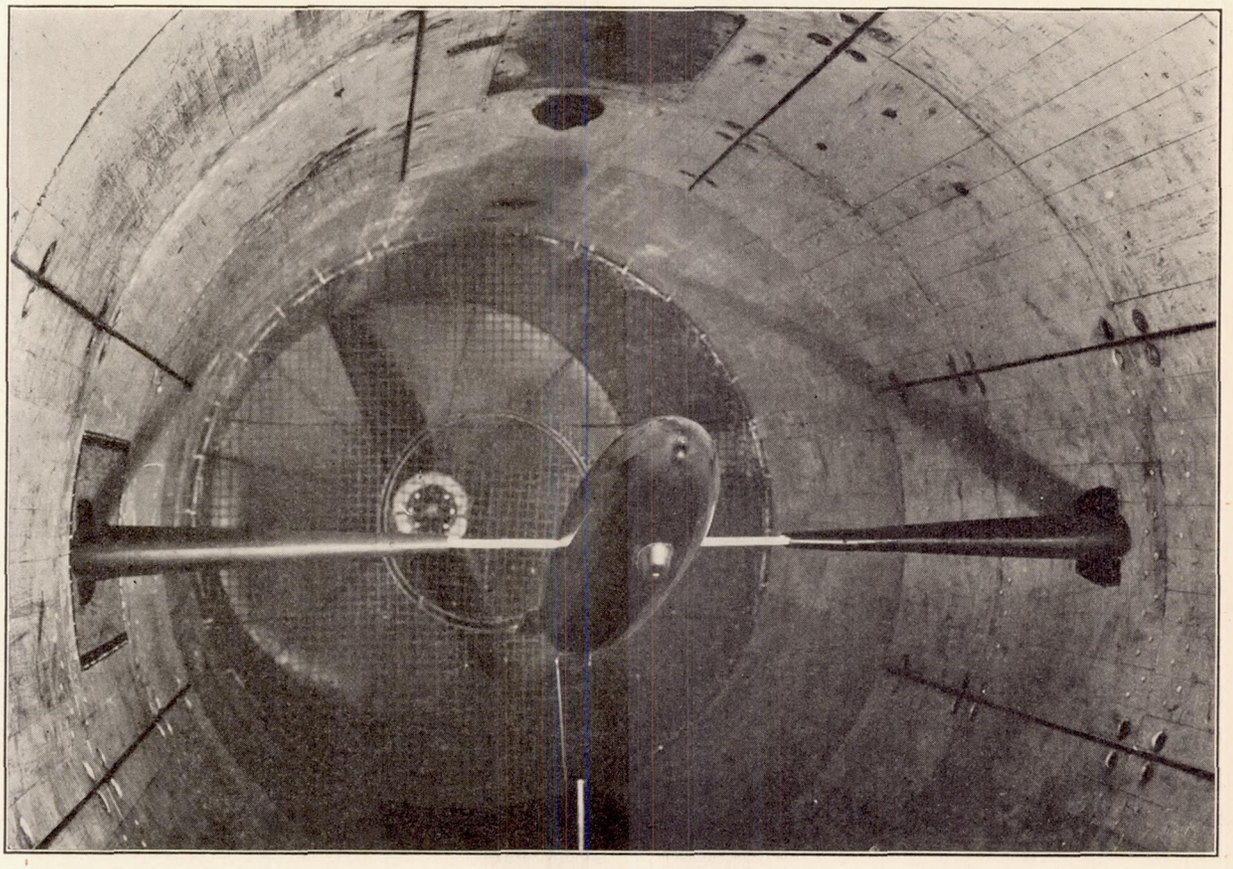

FIGURE 5.—Goodyear-Zeppelin airship model mounted at 20° pitch on the main balance of the closed-throat tunnel

The effects of the last four items had to be evaluated in order to determine the desired forces on the model.

The additional drag on the model due to air-stream convergence was calculated from the formula for an ellipsoid with a volume and fineness ratio equal to that of the model placed in a stream converging in such a manner as to have a linear static pressure gradient. (References 4 and 5.) The formula for this correction is given in the Appendix, and is similar to that for the more conventional horizontal buoyancy correction. However, the actual static pressure gradients of the tunnels were not linear. (Table IV and fig. 9.) The locations of the models in the tunnels are given in Table V. For the open-throat tunnel

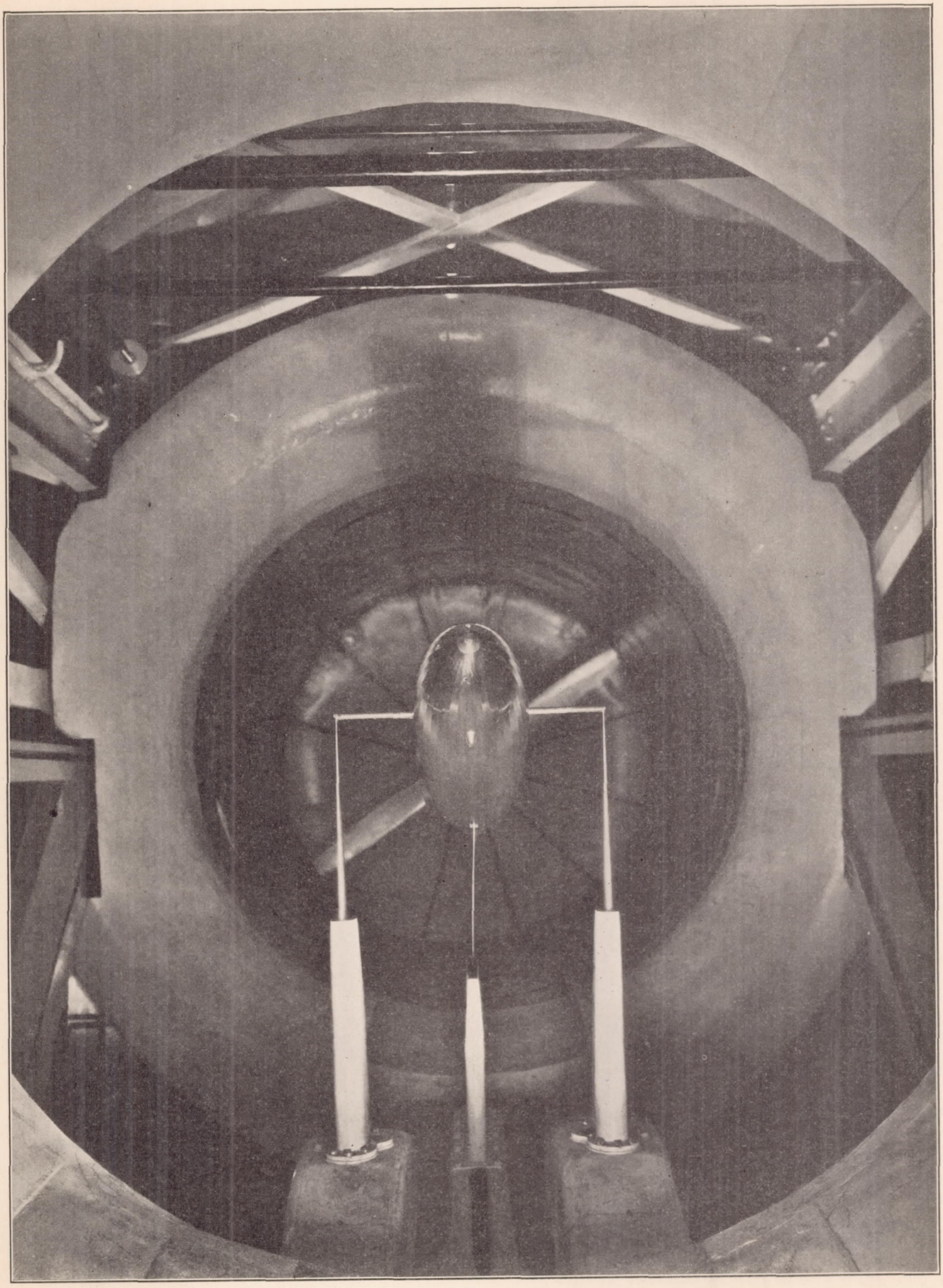

FIGURE 6.—ZRS-4 airship model mounted in pitch on the main balance of the open-throat tunnel

tests, a process of graphical integration was used to arrive at this correction. For the closed-throat tunnel tests the models were divided into three sections and an average linear static pressure gradient was used for each part. These gradients were close approximations to the existing gradients for the sections. These methods have little theoretical justification, but the results justify their use. It is thought that they give closer approximations to the correct results than the usual horizontal buoyancy correction. A check was made by testing one model in the open-throat tunnel in two positions having greatly different static pressure gradients. The gradients in the closed-throat tunnel caused much smaller corrections than those in the open-throat tunnel. The effects of stream convergence on lift and the effects of cross-tunnel static pressure gradients were considered negligible.

The forces due to the main balance model supports, and the interference of the model on the supports were determined in the closed-throat tunnel tests by placing dummy models in the model position so that they did not touch the supports. This force was then measured directly on the balance. The same general procedure was used in the open-throat tunnel tests, except that the model mounted on the auxiliary balance was used instead of the dummy model. The main balance windage was included in the balance readings.

The discrepancy between the results on the main and auxiliary balances in the closed-throat tunnel tests indicates that the corrections for the interference of the main balance model supports on the model were inaccurate. Therefore, in the open-throat tunnel tests, this interference effect was determined by measuring the drag of the model mounted on the auxiliary balance with the main balance model supports in place but not touching the model, and with them removed.

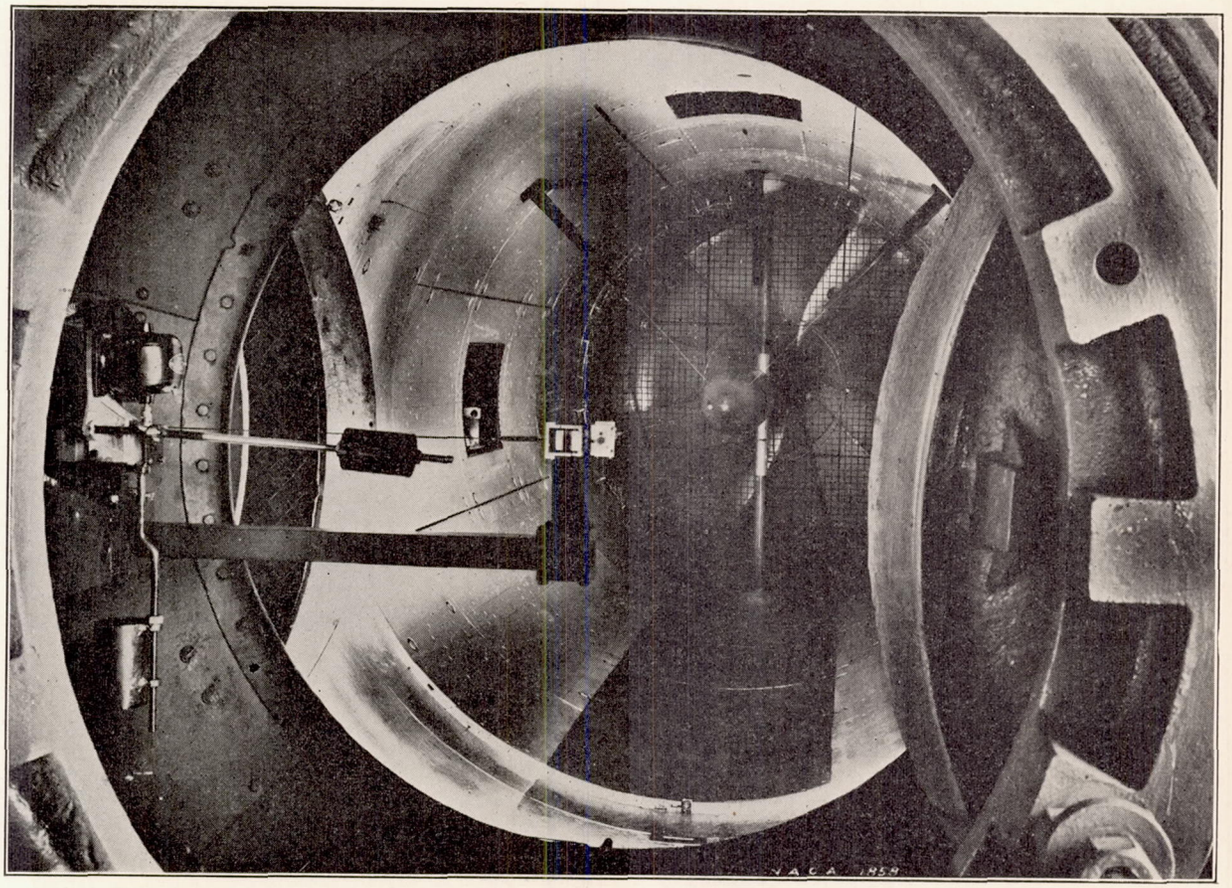

FIGURE 7.—Goodyear-Zeppelin airship model mounted on the auxiliary drag balance in the closed-throat tunnel

The drag of the auxiliary balance model support wires was calculated in the closed-throat tunnel tests. (Reference 6.) The interferences were small because of the location of the wires, and they were neglected. In the open-throat tunnel tests, an attempt was made to determine the wire drag and interferences by measuring the drag of the model mounted on the main balance with and without the auxiliary balance model support wires in place. It was found, however, that this method was subject to considerable error because of the small magnitude of the correction. Consequently, this correction was calculated as in the previous tests.

The formulas used in the calculation of the results are given in the Appendix. It will be noted that the coefficients are based on $(vol)^{\frac{2}{3}}$, and that the Reynolds Numbers are based on the lengths of the models.

TESTS

The models were tested under the following conditions: bare hull, hull with fins, and hull with fins and car. Brass and wooden V-shaped fins were attached to the different models as requested by the Navy Department. Two sizes of cars were attached for the tests on hull with fins and car, a small car being used on the small models and a large one on the large models. The tests were made at tank pressures of 1, 2.5, 5, 10, and 20 atmospheres for the bare-hull condition, and at pressures of 1, 10, and 20 atmospheres for the other conditions. A tabulation of the tests is given in Table VI.

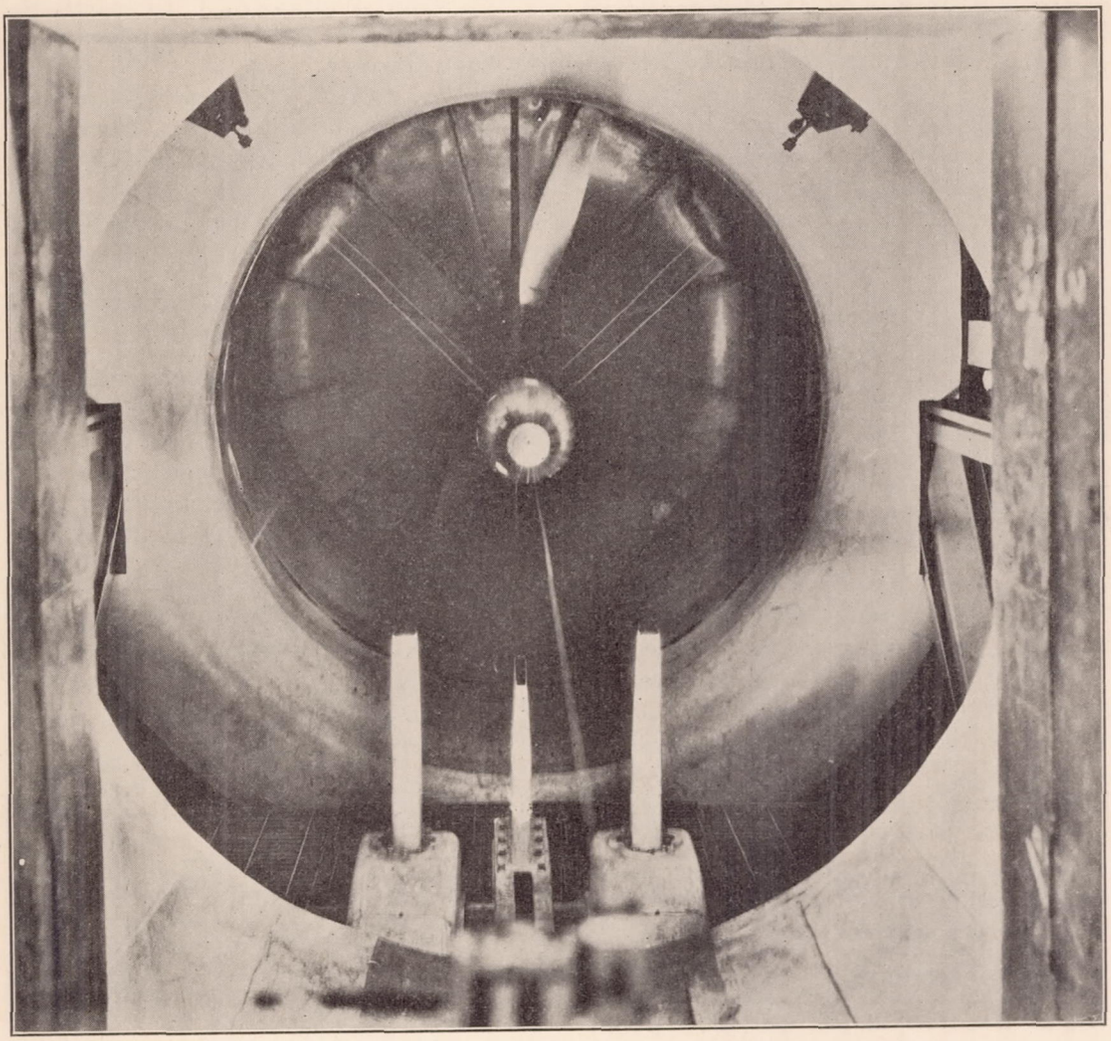

FIGURE 8.—Goodyear-Zeppelin airship model mounted on auxiliary drag balance in the open-throat tunnel

PRECISION

The accuracy of the measured gross forces is believed to be within the following limits except for the lift and moment near zero pitch, which are probably less accurate:

Lift, ±3 per cent.
Moment, ± 5 per cent.
Drag on main balance, ±3 per cent.
Drag on auxiliary balance, ±2 per cent.

The large magnitude of these possible errors was due mainly to an unsteady air stream and to vibrations of the tunnel structure to which the balances were attached. Changes in surface texture between runs caused additional errors, which may be of about the same magnitude as those listed above. The measured corrections were obtained from the difference of measured gross force measurements, and they contain all the above errors.

The accuracy of the calculation of the wire drag for models on the auxiliary balance is believed to be as great as that of the measured corrections. There is an additional error due to the neglected mutual interference of wires and model, but this error probably is small because of the location of the wires. The drag correction for air-stream convergence is thought to be

more nearly accurate than the conventional horizontal buoyancy correction.

No correction has been applied to the lift for the effect of air-stream convergence, and no corrections have been made for the influence of cross-stream static pressure gradients or for wall effects. The errors due to these effects are believed to be less than 1 per cent. The same correction for the effect of air-stream convergence on drag has been applied at all angles of pitch, and this additional drag has been assumed to act at the center of buoyancy of the models for the purpose of moment calculations. The model support and balance windage corrections for any one

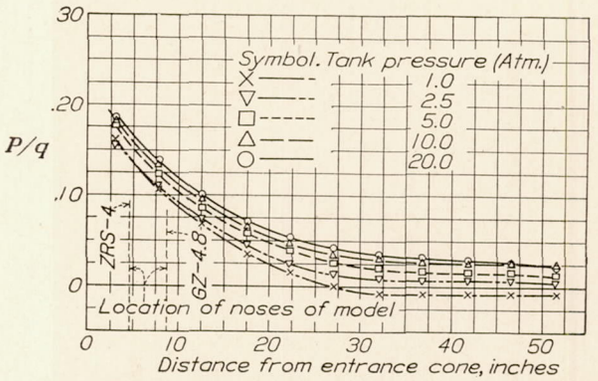

FIGURE 9.—Ratio of static to dynamic pressure on the center line of the open-throat tunnel. Static pressure referred to pressure of still air in test chamber as zero

model have been assumed to be the same for all angles of pitch. These assumptions may have caused appreciable consistent errors.

Figure 10 shows that the agreement between drag coefficients for the GZ–4.8 model as tested in two positions in the open-throat tunnel with greatly different static pressure gradients and in the closed throat tunnel is within ±8 per cent, except at the lowest Reynolds Numbers where air-stream turbulence effects are appreciable. This agreement may be taken as a general indication of the accuracy of the tests.

RESULTS

The results of the tests in pitch of the bare-hull Goodyear-Zeppelin airship models without parallel middle bodies are given in Figure 11. The curves of lift, drag, and moment coefficients at five values of Reynolds Number are plotted against the angle of pitch for the GZ–3.6, GZ–4.8, GZ–6.0, and the GZ–7.2 models. Similar curves for the bare-hull models with parallel middle bodies, namely, the GZ–5.3, GZ–5.6, GZ–5.8, and the GZ–6.8 models, are given in Figure 12, and for the models tested with appendages in Figures 13, 14, and 15. Figure 16 shows similar curves for the GZ–4.8 and the ZRS–4 models, both with and without appendages, as tested in the open-throat tunnel.

The results of the drag tests on the bare-hull models without parallel middle bodies at zero pitch on the auxiliary balance are given in Figure 17 (A). The curves of drag coefficient are plotted against Reynolds Number on logarithmic scales. Similar curves are given for the bare-hull models with parallel middle bodies in Figure 17 (B), and for the models tested with and without appendages in Figure 18. Curves for the GZ–4.8 and ZRS–4 bare-hull models as tested at zero pitch on the auxiliary balance in the open-throat tunnel are given in Figure 19. The results of the close-throat tunnel test on the GZ–4.8 model are also given for comparison.

The results of the tests on effect of surface texture on drag are given in Figure 20. Curves of drag coefficients at zero pitch for the GZ–4.8 bare-hull model with three degrees of surface roughness are plotted on logarithmic scales against Reynolds Number. The curves show greatly increased drag resulting from increased surface roughness.

DISCUSSION

Pitch.—The effect of pitch on the aerodynamic characteristics of the models is shown in Figures 11 to 16, inclusive. The lift and moment at zero pitch are not exactly zero because of air flow and model eccentricity. The lift coefficient increases to values of about 0.10 to 0.12 for the bare-hull models at 15° positive pitch, and

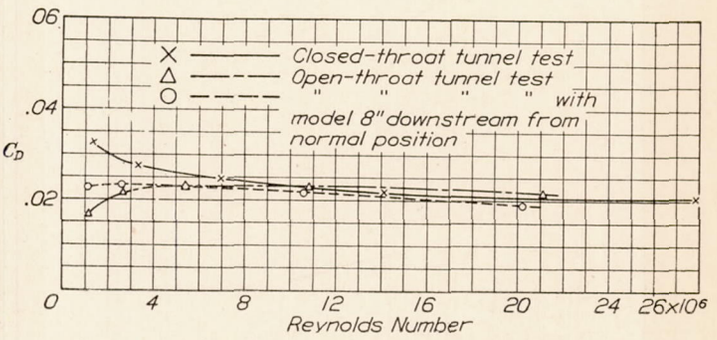

FIGURE 10.—Drag coefficients of the Goodyear-Zeppelin airship model. Fineness ratio, 4.8; zero pitch; bare hull

to values of about 0.25 to 0.35 for the models at the same attitude with fins and cars.

The moment coefficients for the bare-hull models increase from approximately zero at zero pitch to a value of about 0.06 to 0.08 at 15° positive pitch. The theoretical moment coefficients have been calculated from the values of $K_2 - K_1$ (reference 7) given in Figure 21, and Figure 22 shows the ratio of the actual to the theoretical moment coefficients plotted against angle of pitch. This ratio is about 0.70 at the larger angles where the erros due to eccentricity are unimportant. This value is the one usually found for this ratio. (Reference 7.) The moment coefficients for the models with fins and cars, and with fins only, increase with increasing pitch to a maximum at an angle of roughly

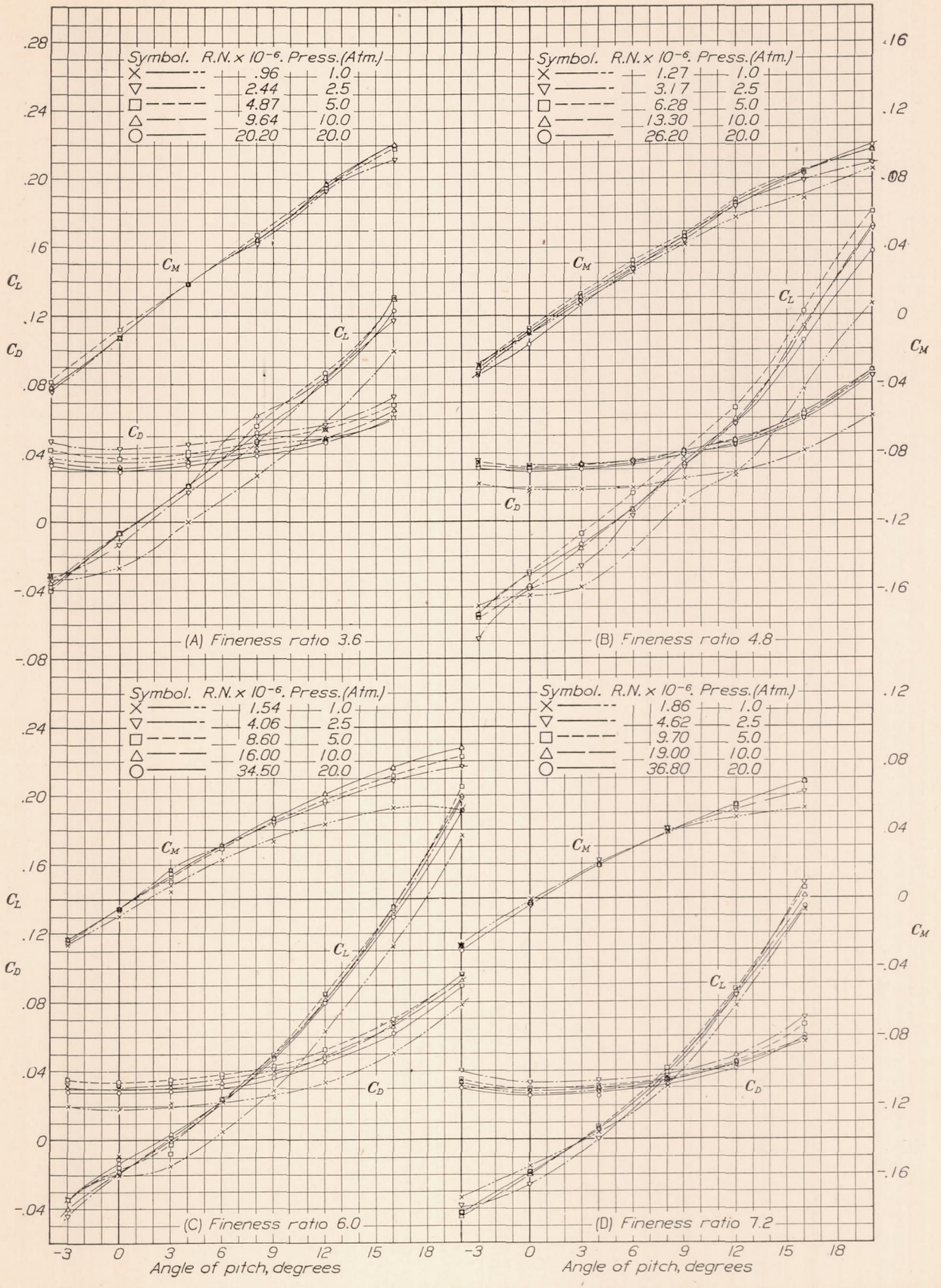

FIGURE 11.—Aerodynamic characteristics of Goodyear-Zeppelin airship models. Bare hull without parallel middle bodies. Tested in closed-throat tunnel

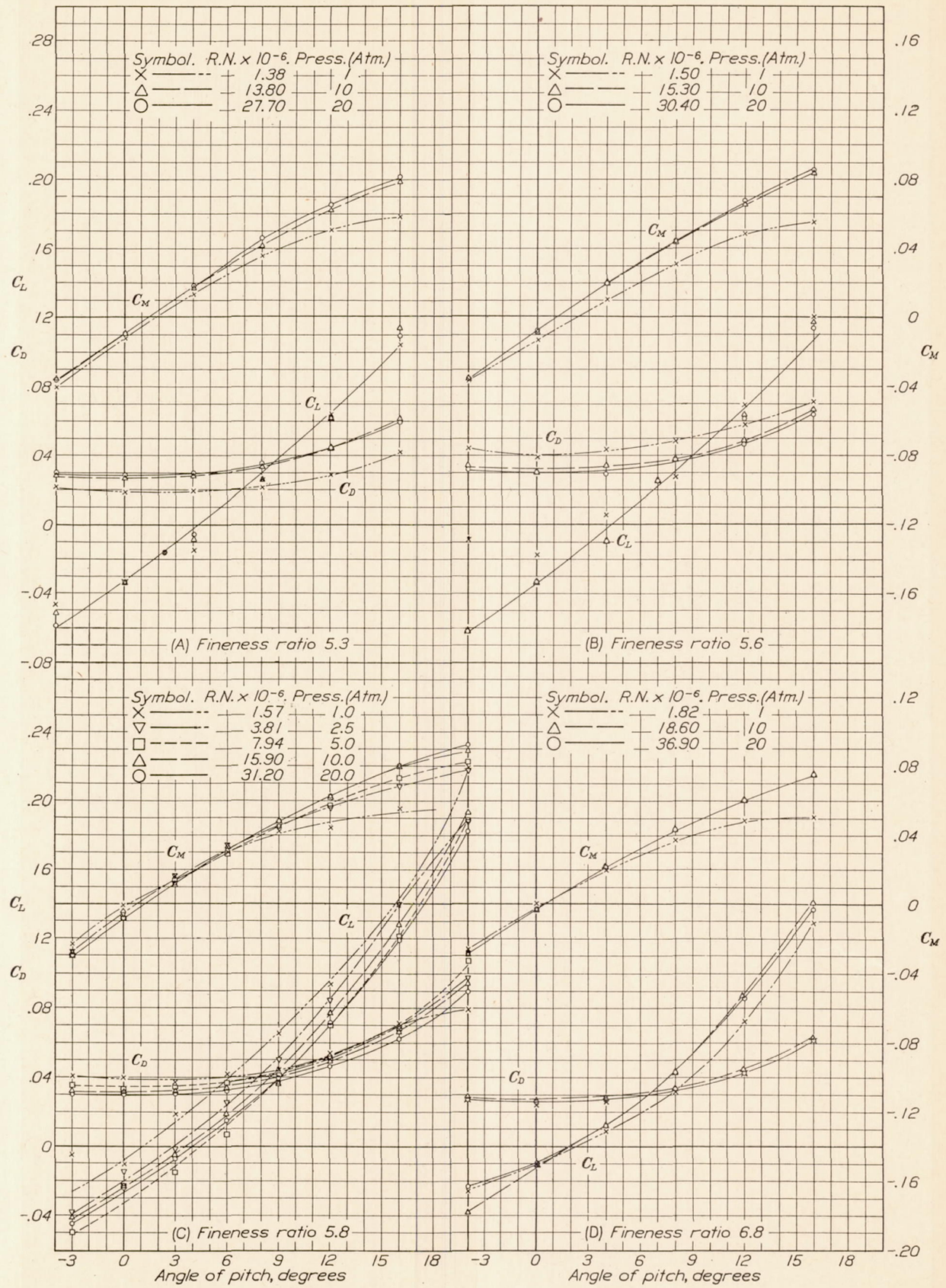

FIGURE 12.—Aerodynamic characteristics of Goodyear-Zeppelin airship models. Bare hull with parallel middle bodies. Tested in the closed-throat tunnel

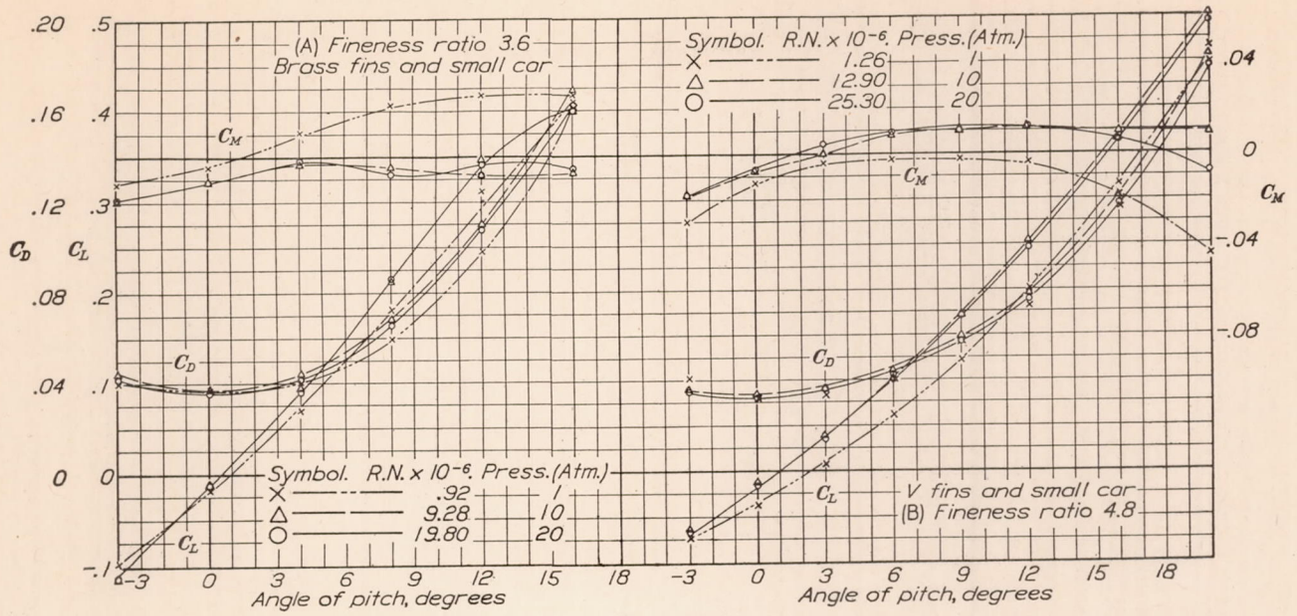

FIGURE 13.—Aerodynamic characteristics in pitch of the GZ–3.6 and GZ–4.8 airship models with fins and car. Tested in the closed-throat tunnel

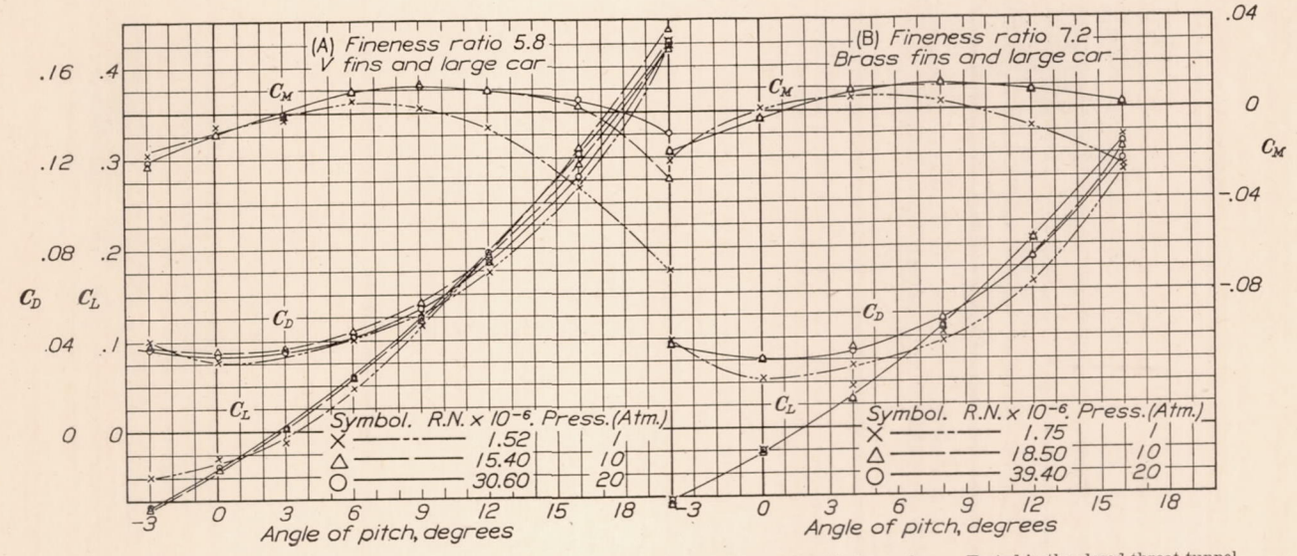

FIGURE 14.—Aerodynamic characteristics in pitch of the GZ–5.8 and GZ–7.2 airship models with fins and car. Tested in the closed-throat tunnel

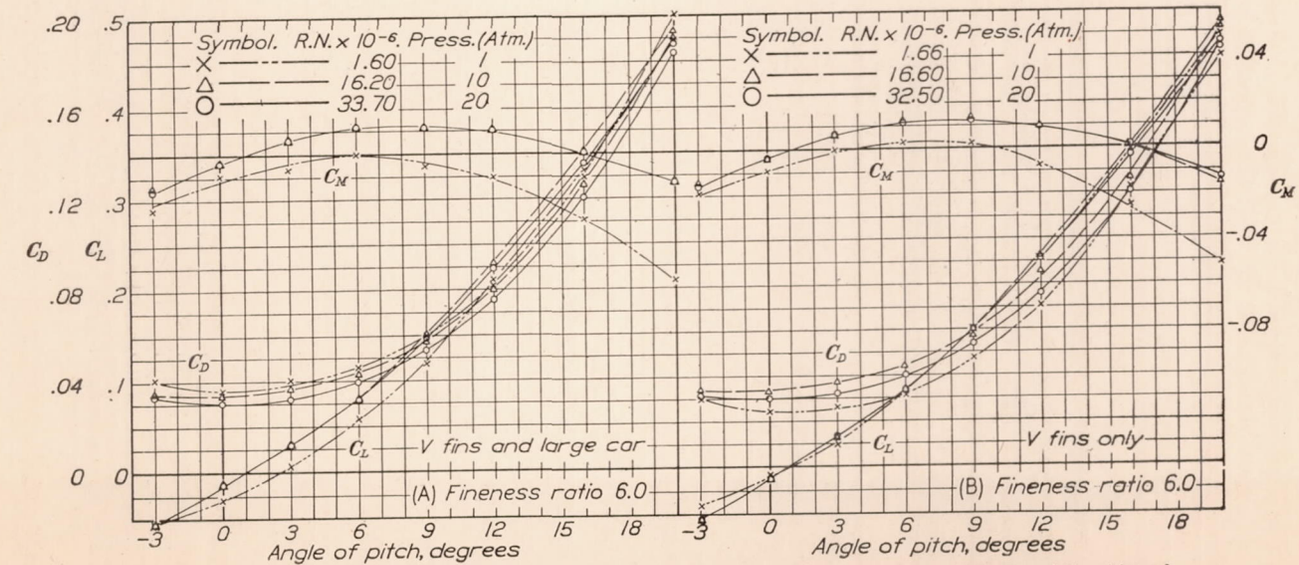

FIGURE 15.—Effect of car on aerodynamic characteristics of the GZ–6.0 model in pitch. Tested in the closed-throat tunnel

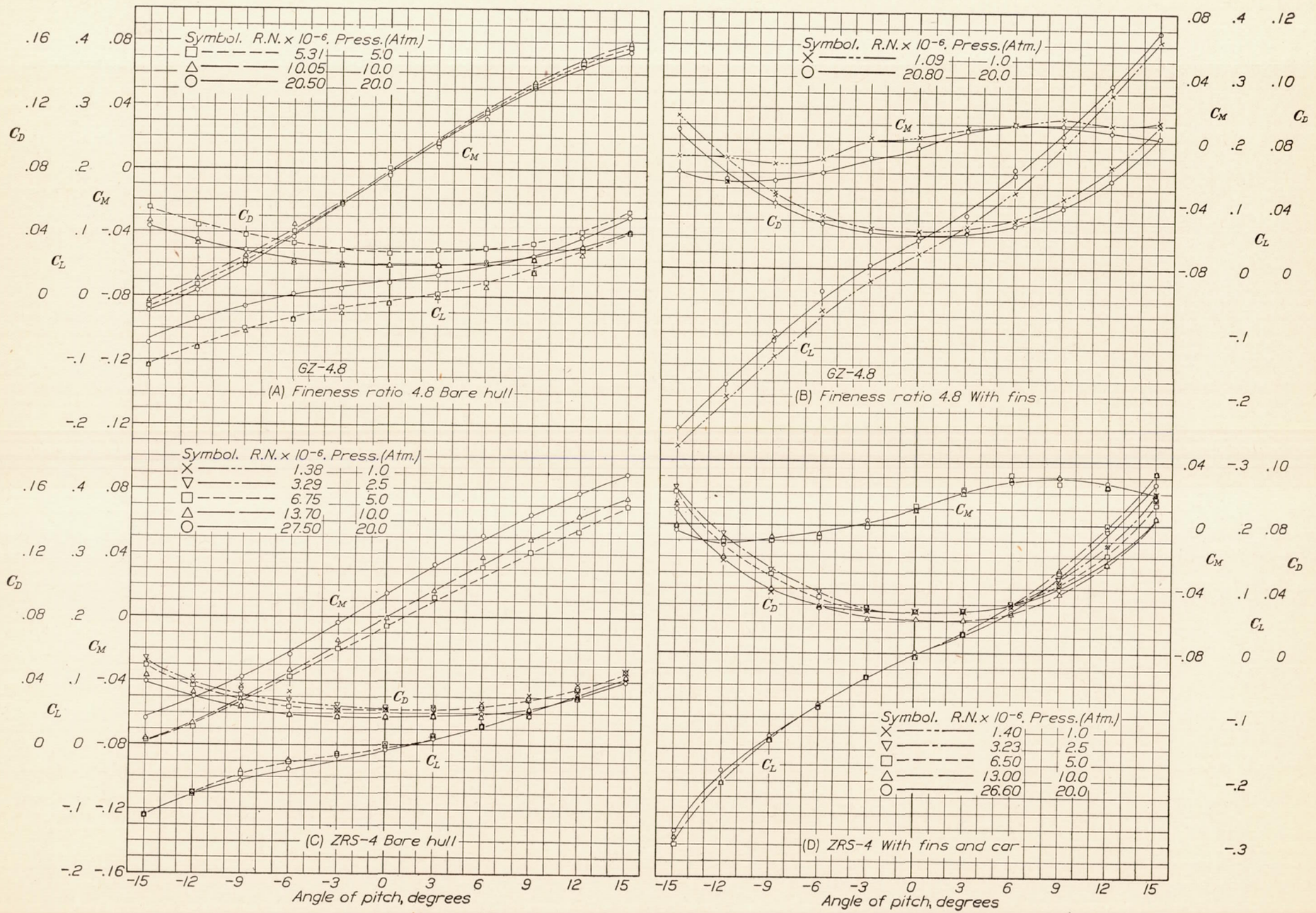

FIGURE 16.—Aerodynamic characteristics in pitch of the GZ-4.8 and ZRS-4 airships models as tested in the open-throat tunnel, with and without appendages

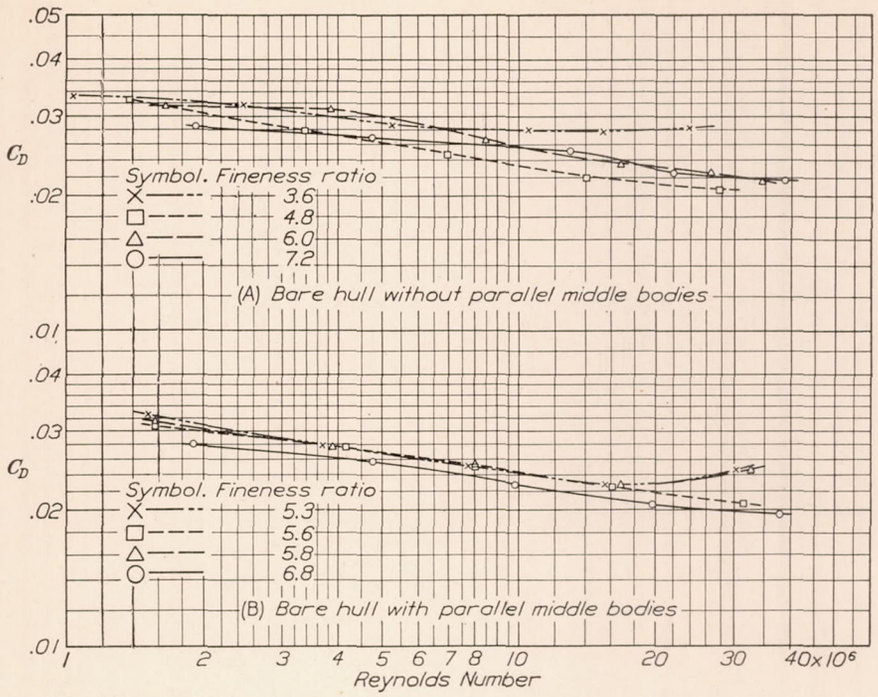

FIGURE 17.—Drag coefficient of Goodyear-Zeppelin airship models. Bare hull, 0° pitch. Tested in the closed-throat tunnel

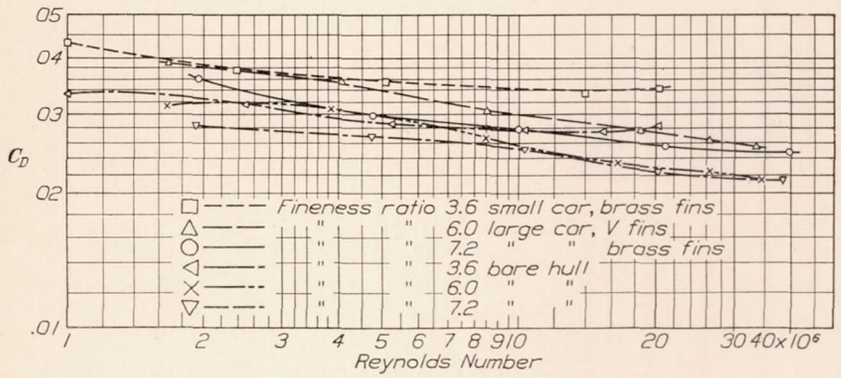

FIGURE 18.—Drag coefficient of Goodyear-Zeppelin models; 0° pitch, closed-throat tunnel, with and without appendages

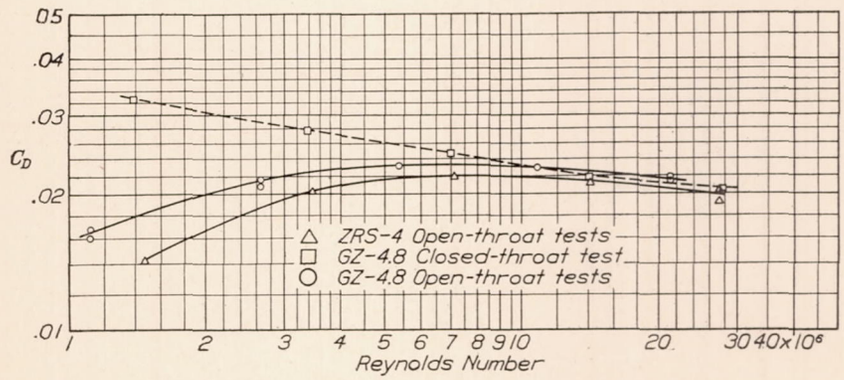

FIGURE 19.—Drag coefficients of GZ-4.8 and ZRS-4 airship models. Bare hull models

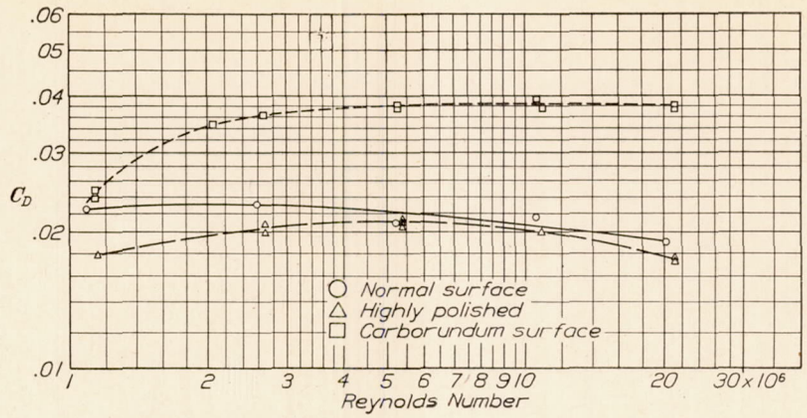

FIGURE 20.—Effect of surface roughness on drag. Drag coefficients of Goodyear-Zeppelin airship model. Angle of pitch 0°; bare hull; fineness ratio, 4.8; model 8 inches downstream from normal position in open-throat tunnel

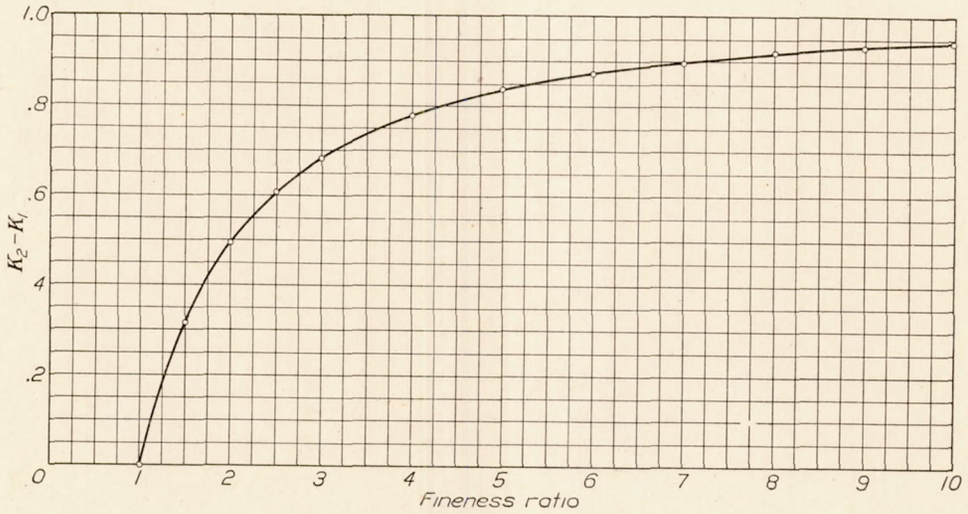

FIGURE 21.—Coefficient of apparent additional transverse and longitudinal mass for ellipsoids

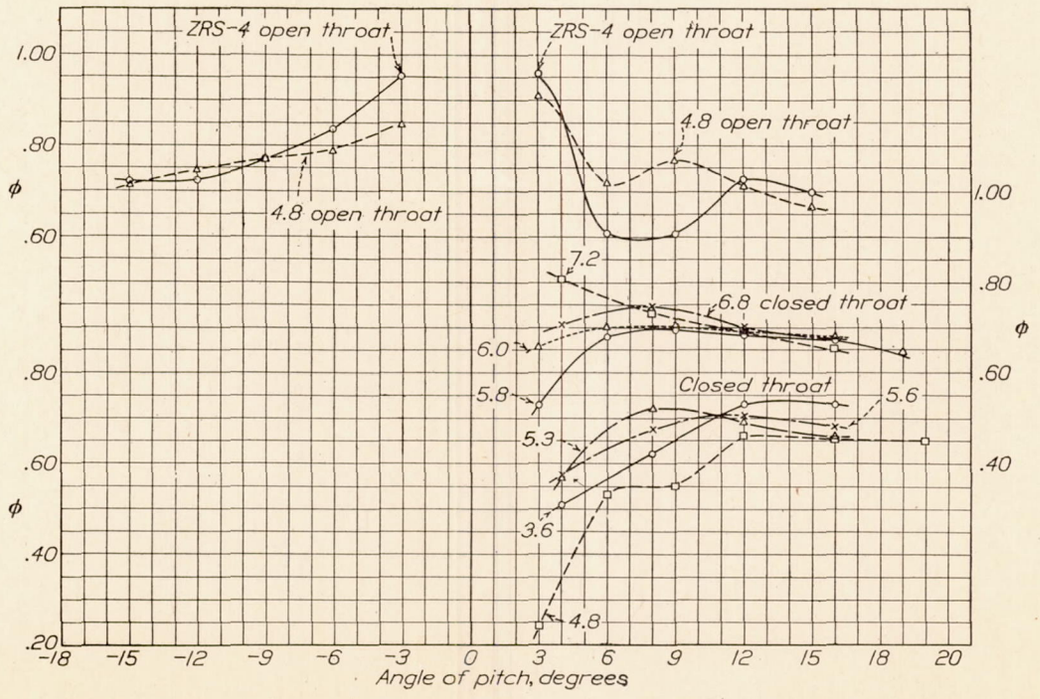

FIGURE 22.—Ratio of experimental to theoretical moment coefficients. Bare hull models; 20 atmosphere tank pressure

9°, above which the slope of the moment curve becomes negative.

The drag coefficients are least at zero pitch. The rate of increase with pitch is small at small angles of pitch, but it becomes greater as the pitch increases.

Fins and cars.—The magnitude of all effects of fins and cars upon the aerodynamic characteristics of airships is dependant mainly upon the relative sizes of the hull and appendages. Consequently, it is impossible to compare directly the effects on the different models because the relative sizes vary. The influence of the fins and cars for the combinations tested can be seen from a comparison of Figures 11 and 12 with Figures 13, 14, and 15, and from Figures 16 and 23. The lift is increased at positive angles of pitch. The moment due to the fins and car of the GZ–6.0 model is shown in Figure 24. The appendages cause a decrease in moment when the ship is in positive pitch.

The increase in drag due to appendages with the model at zero pitch is shown in Figure 18 to be from 15 to 20 per cent of the bare-hull drag at the larger Reynolds Numbers and more at the smaller Reynolds Numbers. This increase is greater at larger angles of pitch and is about 100 per cent at 15°, except for the GZ–3.6 model, which shows an increase of about 150 per cent of the bare-hull drag at that attitude.

Tests on the GZ–6.0 model (figs. 15 and 24 with fins and car, and with fins only, show that the car has no effect on lift and moment within the accuracy of the tests, and only a slight effect on drag.

Fineness ratio.—Fineness ratio is defined for the purpose of this report as the ratio of the major axis of the airship to its greatest diameter. An airship with a fineness ratio near unity would have a very large pressure drag. If only airships of good shape are considered, that part of the drag coefficient due to pressure drag is greatly decreased as the fineness ratio is increased; but, if the increase is continued, a point is reached where the decrease in the pressure drag coefficient is too small to be appreciable. That part of the drag coefficient due to skin friction is increased as the fineness ratio is increased, because the ratio of

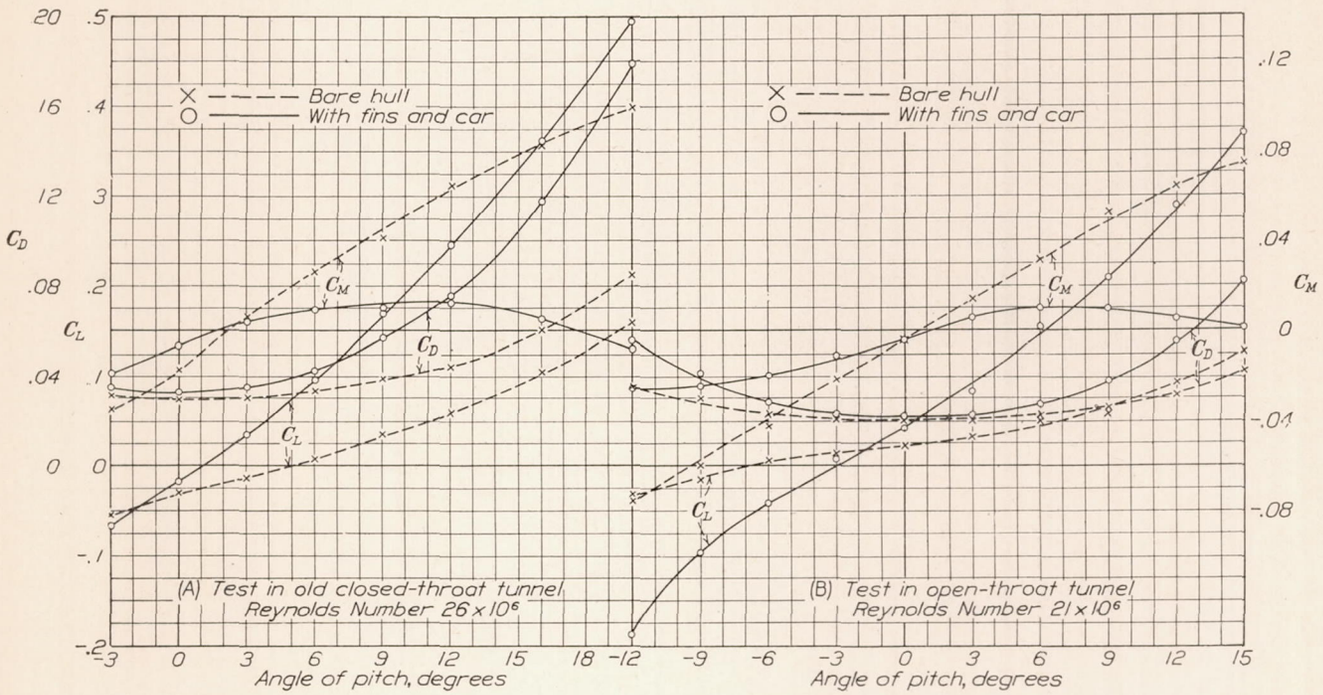

FIGURE 23.—Aerodynamic characteristics in pitch of the GZ–4.8 airship model as tested with and without appendages in the closed and open throat tunnels

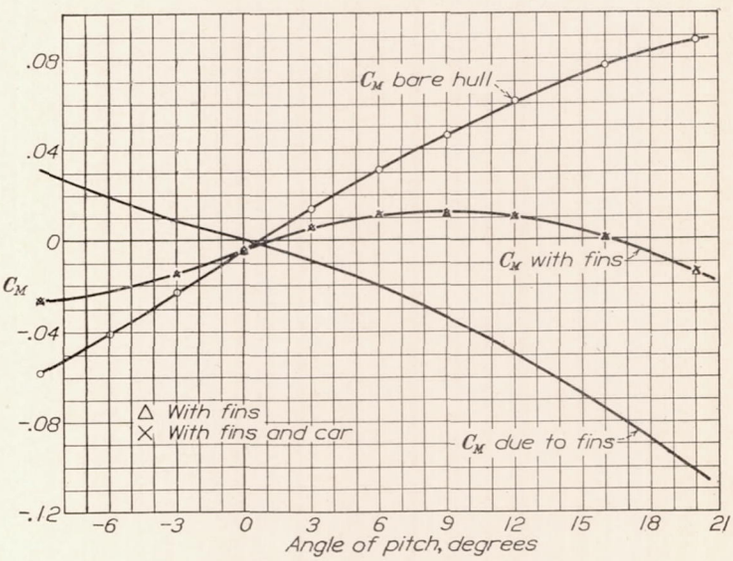

FIGURE 24.—Moment due to fins or fins and car. Goodyear-Zeppelin airship model. Fineness ratio, 6.0; Reynolds Number 33×10^6

surface area to volume is increased. It follows that for airships with the same generating curve, there will be a definite fineness ratio at which the drag coefficient will be a minimum, although there may be little increase in drag for airships with fineness ratios varying somewhat from the one giving minimum drag. Figure 25 (A) shows that there is actually little difference in the drag coefficients of the models with fineness ratios between 4.8 and 7.2. The scattering of the points is due to the inclusion of models with parallel middle bodies, to inaccuracies of measurement, and also, very likely, to different test conditions causing differences in the boundary-layer flow.

If an airship form is used for the fairing of objects, the important drag coefficient is one based on the maximum cross-sectional area instead of on $(\text{vol})^{\frac{2}{3}}$. In Figure 25 (B) this coefficient (C_{D_A}) is shown plotted against fineness ratio for the Goodyear-Zeppelin bare-hull models at a Reynolds Number of 20,000,000. The results indicate that C_{D_A} is a minimum for this generating curve at a fineness ratio of about 4.5.

These tests show no consistent variation of lift coefficient with fineness ratio, either for the models with the same generating curve or for those with parallel middle bodies. (Fig. 26.) In general, the lift coefficients are higher for the models with the larger fineness ratios, but this variation is small and not very systematic.

The moment coefficients are higher for the bare-hull models with the smaller fineness ratios (fig. 27); but this effect is not entirely systematic, probably because all the models do not have the same generating curve. From consideration of the theoretical moments, the moment coefficients of the Goodyear-Zeppelin bare-hull models would be expected to increase as the fineness ratio is decreased. The following table gives the theoretical and actual moment coefficients of these models expressed as a function of the pitch. (Reference 7.)

C_m AS A FUNCTION OF THE PITCH

Fineness ratio	Theoretical	Actual (From point: $\alpha=16°$ tank pressure = 20 atmospheres)
3.6	0.258 sin 2α	0.189 sin 2α
4.8	.237 sin 2α	.155 sin 2α
[1]5.3	.230 sin 2α	.152 sin 2α
[1]5.8	.224 sin 2α	.151 sin 2α
6.0	.215 sin 2α	.145 sin 2α
[1]6.8	.210 sin 2α	.142 sin 2α
7.2	.197 sin 2α	.129 sin 2α

[1] Models with parallel middle bodies

Surface roughness.—The large increase in drag coefficient for the GZ–4.8 bare-hull model due to increase in surface roughness is shown in Figure 20. At the highest Reynolds Numbers reached, the drag coefficient for the model coated with No. 180 carborundum is 200 per cent of the drag coefficient for the model with a normal rubbed-varnish surface, and this coefficient for the model with a highly polished surface is 93 per cent of that for the normal model. Although the carborundum surface is far rougher than anything that would be obtained in practice, the large magnitude of the effect of surface roughness makes it imperative thae consideration be given to the condition of the surfact of the model in any interpretation of airship model tests.

Reynolds Number.—The effect of Reynolds Number on the lift and moment coefficients is shown in Figures 11 to 16, inclusive. There is no consistent variation of lift coefficient with Reynolds Number, probably because the data are not sufficiently accurate to show this effect, which is small. Most of the models show an appreciable increase in the moment coefficient at large Reynolds Numbers. This increase is greater for the models equipped with fins and cars than for the bare-hull models.

The drag coefficients for the models in pitch do not show any consistent variation with Reynolds Number. This fact is probably due to the inaccuracy of the results. The drag coefficients at zero pitch for the models tested in the closed-throat tunnel decrease with increasing Reynolds Number (figs. 17 and 18), but the decrease is not systematic for all models. The rate of decrease is greater at small than at large Reynolds Numbers, especially for the models equipped with fins and cars, and the curves of drag coefficients of the bare-hull models plotted against Reynolds Numbers approximate straight lines when plotted on logarithmic scales. The apparently high drag coefficients shown by some of the models at the highest Reynolds Number reached may have been due to the use of insufficient counterweight to keep those models steady at 20 atmospheres tank pressure. The drag coefficients for both models tested in the open-throat tunnel at zero pitch increase at low Reynolds Numbers and decrease at high Reynolds Numbers. (Fig. 19.)

Initial degree of air-stream turbulence.—The drag of airship hulls with good forms is very largely due to skin friction. Pressure distribution tests on airships and models have repeatedly shown very small pressure drag coefficients. The magnitude of the skin friction, and hence the magnitude of the drag coefficient for the airship, are dependent upon the type of flow existing in the boundary layer. The type of flow depends not only upon the scale, but also upon the steadiness of the air approaching the airship, or, to state this differently, upon the initial degree of air-stream turbulence. The boundary-layer flow is also partly dependent upon the shape of the airship.

The following equation of Blasius expresses the average skin-frictional drag coefficient for all laminar boundary-layer flow on rectangular flat plates. (References 8 and 9):

$$C_F = 1.34R^{-\frac{1}{2}}$$

Burgers and Hansen have established this equation as a good approximation to experimental values. Prandtl's equation

$$C_F = 0.074R^{-\frac{1}{5}}$$

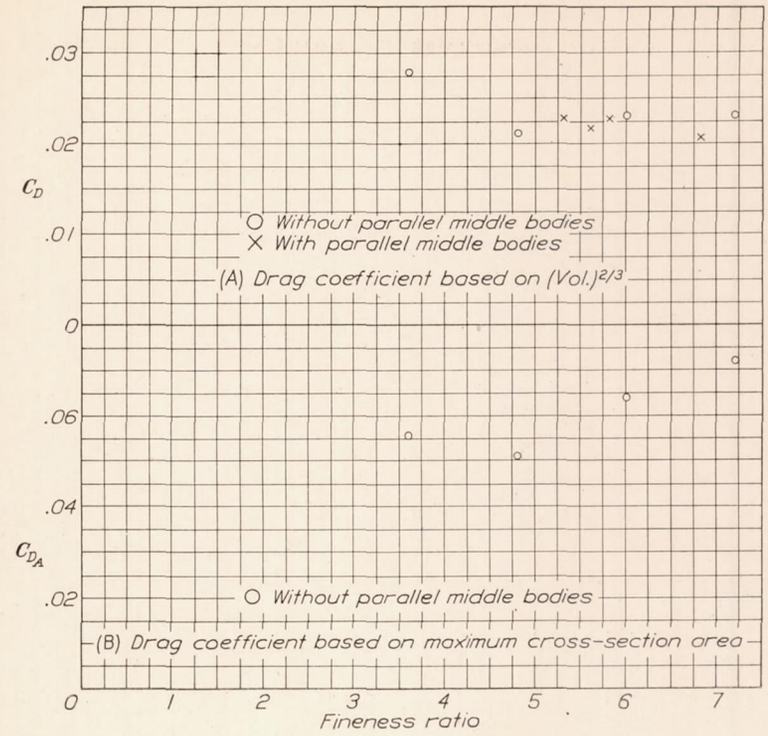

FIGURE 25.—Effect of fineness ratio on drag coefficient at zero pitch. Goodyear-Zeppelin airship models. Bare hulls

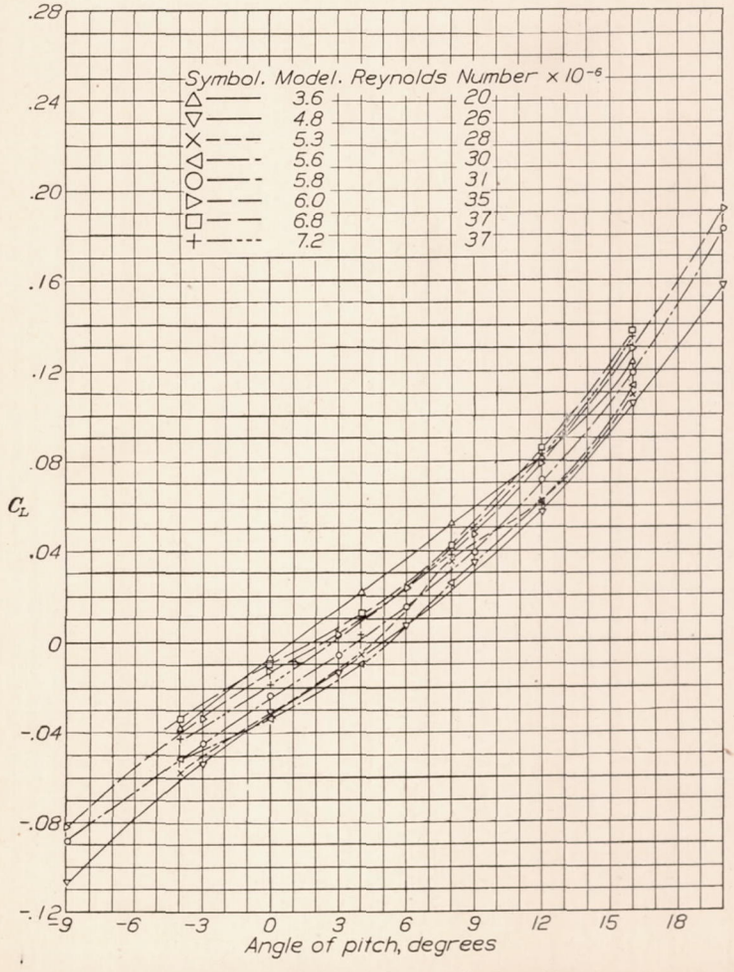

FIGURE 26.—Effect of fineness ratio on lift coefficient. Goodyear-Zeppelin airship models. Lift coefficients at 20 atmospheres: bare hull; tested in the closed-throat tunnel

expresses the average skin-frictional drag coefficient for all eddying boundary-layer flow on rectangular flat plates. (Reference 10.) Curves of C_F are plotted on logarithmic scales against Reynolds Number in Figure 28.

As explained in the above references, the laminar type of boundary-layer flow exists only at small Reynolds Numbers; and, if the Reynolds Number is increased, the flow in the boundary layer becomes eddying on the surface of the downstream portion of the plate, and the transition line between the two types of flow progresses upstream. In wind tunnel tests the Reynolds Numbers are such that the flow is neither entirely laminar nor so largely eddying that the laminar upstream portion can be neglected. Under these conditions the skin-frictional drag coefficient lies on a transition curve between the two curves described above.

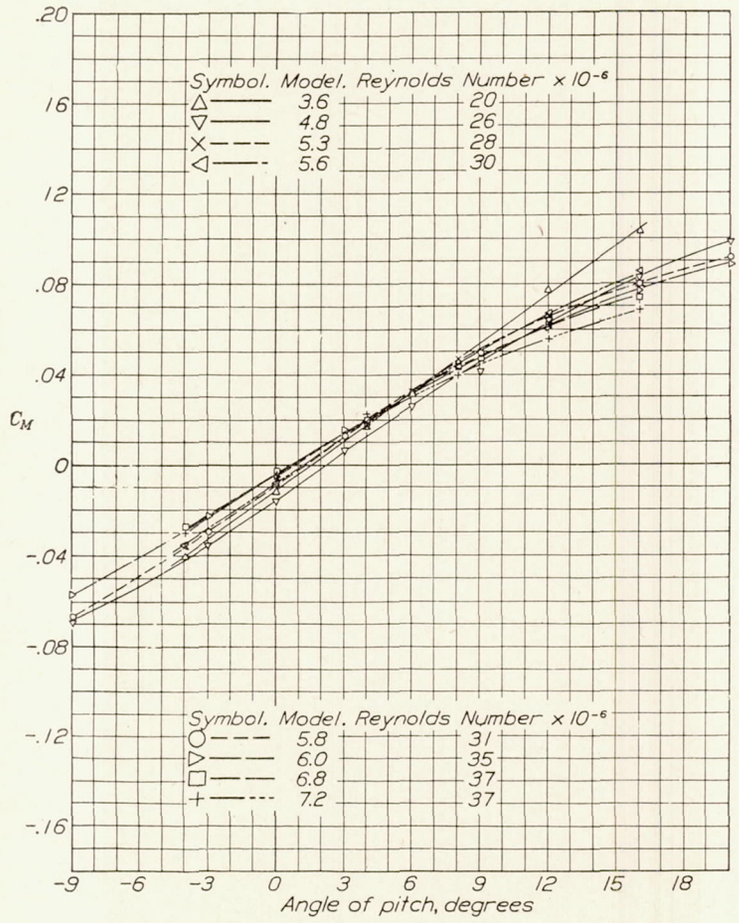

FIGURE 27.—Effect of fineness ratio on moment coefficient. Goodyear-Zeppelin airship models. Moment coefficients at 20 atmospheres; bare hull; tested in the closed-throat tunnel

The value of the Reynolds Number at which the transition from laminar to eddying flow takes place in any given case is called the critical Reynolds Number. The scale at the transition line, i. e., the critical Reynolds Number, may be expressed by R_X in which the characteristic length is the distance from the line to the upstream edge of the plate. The value of the critical Reynolds Number is dependent upon the initial degree of air-stream turbulence (References 9 and 11), and decreases as the initial turbulence increases. The usual values of R_X for wind tunnel work are very roughly 100,000 to 3,000,000.

The transition curve of the skin-frictional drag coefficient can be calculated approximately for a flat plate and a value of the critical Reynolds Number. The following assumptions give two limiting transition curves between which the true curve must lie. (Reference 9.)

1. The laminar flow does not affect the eddying flow behind it at all.
2. The eddying portion over the rear of the plate acts as though the layer were eddying over the whole plate.

Two typical transition curves for rectangular flat plates have been calculated for a critical Reynolds Number of 600,000, and have been plotted in Figure 28.

The total drags of some of the airship models have been expressed in the form of skin-frictional drag coefficients (C_{F_D}). This coefficient is based on the surface areas of the models. The inclusion of the pressure drag is not very important because this drag is comparatively small, and probably varies little with the Reynolds Number. Curves of this coefficient are plotted against Reynolds Number in Figure 28 for the GZ–4.8 model as tested in the old closed-throat tunnel, and as tested in two positions with three degrees of surface roughness in the open-throat tunnel. The curve for the GZ–7.2 model is also included.

The figure shows that the curves for the models tested in the open-throat tunnel resemble transition curves for rectangular flat plates at the lower Reynolds Numbers, and closely approximate the curve for all eddying boundary-layer flow at the higher Reynolds Numbers. The curves from the closed-throat tunnel tests lie nearly parallel with those for all eddying boundary-layer flow on flat plates. The turbulence in this tunnel was much greater than that in the open-throat tunnel (reference 2), and the critical Reynolds Number was apparently so far below the test range that the curves show no resemblance to transition curves at the lower Reynolds Numbers.

Recommendations for future work.—The curves of the drags of airship models, when expressed as skin-frictional drag coefficients, resemble the curves for skin friction on flat plates. The indications are that much may be done to predict full-scale drag coefficients of airship models from separate evaluations of pressure and friction drags. In order to calculate the friction drags it will be necessary to make experiments to determine the effect of pressure gradients, curva-

ture, and taper of a body of revolution upon the boundary layer. This work should be undertaken in conjunction with an extensive study of turbulence. Although the determination of turbulence by plots of sphere or streamline-body tests has been used fairly successfully, this method is subject to error because the assumption is made that the turbulence is constant, whereas it probably varies with Reynolds Number. The work should be combined with complete boundary-layer surveys, force tests, and pressure-distribution tests on an airship model, and, if possible, on the full-sized airship.

2. The drag coefficients for the airship models with the Goodyear-Zeppelin generating curve vary little between fineness ratios of 4.8 and 7.2.

3. Wind tunnel tests of airship models may lead to erroneous conclusions because of the effect of the initial degree of air-stream turbulence, and because of differences in surface roughness.

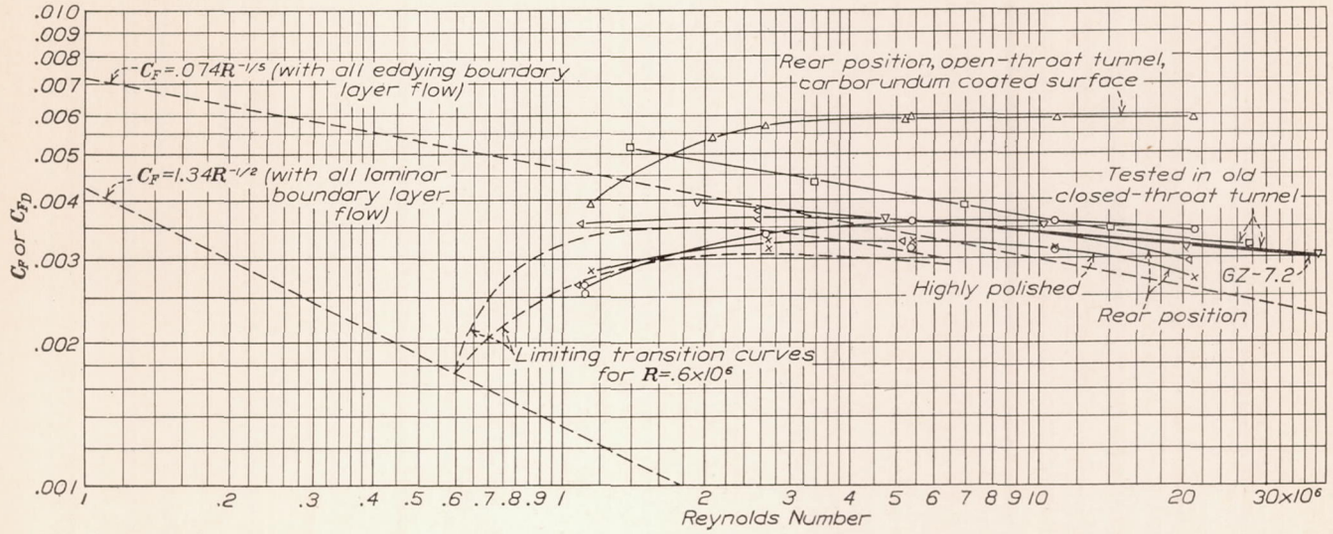

FIGURE 28.—Comparison of skin friction on airship models and rectangular flat plates. Dashed lines represent theoretical curves for skin friction on rectangular flat plates. Solid lines represent test results on bare-hull airship models. These curves are for the GZ–4.8 model tested in the normal position with normal surface in the open-throat tunnel except as noted

4. The variation of the resistance of airship models at the large Reynolds Numbers obtained in these tests is apparently a determinable function of the Reynolds Number.

CONCLUSIONS

1. The addition of fins and cars to airship models in the combinations tested increases the drag from 15 to 20 per cent at zero pitch.

LANGLEY MEMORIAL AERONAUTICAL LABORATORY,
NATIONAL ADVISORY COMMITTEE FOR AERONAUTICS,
LANGLEY FIELD, VA., *January 27, 1931.*

APPENDIX

$C_L = \frac{L}{q(\text{vol})^{\frac{2}{3}}}$, lift coefficient.

$C_M = \frac{M}{ql(\text{vol})^{\frac{2}{3}}}$, moment coefficient.

$C_D = \frac{D}{q(\text{vol})^{\frac{2}{3}}}$, drag coefficient.

$C_{D_A} = \frac{D}{qA}$, drag coefficient based on maximum cross-sectional area.

$C_F = \frac{F}{qS}$, skin frictional drag coefficient.

$C_{F_D} = \frac{D}{qS}$, skin frictional drag coefficient based on assumption total drag is skin frictional.

$R = \frac{\rho Vl}{\mu}$, Reynolds Number.

$R_X = \frac{\rho VX}{\mu}$, Reynolds Number at point (X).

$C_M' = \frac{(K_2 - K_1)\ (\text{vol})^{\frac{1}{3}} \sin 2\alpha}{l}$, theoretical moment coefficient about center of buoyancy.

$\phi = \frac{C_M}{C_M'}$

$C_D' = \frac{(\text{vol})_1' \frac{dp}{dx}}{q(\text{vol})^{\frac{2}{3}}}$, drag coefficient due to stream convergence.

$(\text{vol})_1' = (\text{vol}) + (\text{vol})_1''$.

$(\text{vol})_2' = (\text{vol}) + (\text{vol})_2''$.

$K_1 = \frac{(\text{vol})_1''}{(\text{vol})}$.

$K_2 = \frac{(\text{vol})_2''}{(\text{vol})}$.

Where

L, lift.

M, moment about center of buoyancy.

D, drag.

F, force due to skin friction.

α, angle of pitch in degrees.

l, length of model.

A, maximum cross-sectional area of model normal to axis.

S, total surface area.

d, distance downstream along axis of tunnel measured from selected stations.

X, distance downstream measured from upstream edge of plate.

V, air speed.

p, static pressure.

q, dynamic pressure.

ρ, mass density of the fluid.

μ, coefficient of viscosity.

(vol), volume of model.

$(\text{vol})_1'$, virtual volume of the body placed longitudinally in an accelerating stream

$(\text{vol})_2'$, virtual volume of the body placed transversely in an accelerating stream.

$(\text{vol})_1''$, apparent additional volume of the body placed longitudinally in an accelerating stream.

$(\text{vol})_2''$, apparent additional volume of the body placed transversely in an accelerating stream.

REFERENCES

1. Munk, Max M., and Miller, Elton W.: The Variable Density Wind Tunnel of the National Advisory Committee for Aeronautics. N. A. C. A. Technical Report No. 227, 1926.
2. Jacobs, Eastman N.: Sphere Drag Tests in the Variable Density Wind Tunnel. N. A. C. A. Technical Note No. 312, 1929.
3. Higgins, George J.: Tests of the N. P. L. Airship Models in the Variable Density Wind Tunnel. N. A. C. A. Technical Note No. 264, 1927.
4. Taylor, G. I.: The Force Acting on a Body Placed in a Curved and Converging Stream of Fluid. British A. R. C. R&M No. 1166, 1928.
5. Lamb, H.: Notes on the Forces Experienced by Ellipsoidal Bodies Placed Unsymmetrically in a Converging or Diverging Stream. British A. R. C. R&M No. 1164, 1928.
6. DeFoe, George L.: Resistance of Streamline Wires. N. A. C. A. Technical Note No. 279, 1928.
7. Munk, Max M.: The Aerodynamic Forces on Airship Hulls. N. A. C. A. Technical Report No. 184, 1924.
8. Blasius, H.: Zeitschrift für Mathematik und Physik. 56, 1908, p. 1.
9. Jones, B. M.: Skin Friction and the Drag of Streamline Bodies. British A. R. C. R&M No. 1199, 1928.
10. Prandtl, L., and Betz, A.: Ergebnisse der Aerodynamischen Versuchsanstalt zu Göttingen. 111 Liefrung, 1927, p. 1.
11. Dryden, H. L., and Keuthe, A. M.: Effect of Turbulence in Wind Tunnel Measurements. N. A. C. A. Technical Report No. 342, 1930.

TABLE I

ORDINATES OF THE GOODYEAR-ZEPPELIN AIRSHIP CURVE

Station, per cent length from nose	Ordinates	Station, per cent length from nose	Ordinates
	Inches		*Inches*
0.000	0.000	53.00	3.780
0.438	0.752	56.65	3.738
0.63	1.623	60.30	3.667
5.55	2.264	63.95	3.590
9.20	2.758	67.60	3.470
12.85	3.108	71.25	3.315
16.50	3.358	74.90	3.127
20.15	3.533	78.55	2.902
23.80	3.653	82.20	2.630
27.45	3.730	85.85	2.313
31.10	3.775	89.50	1.937
34.75	3.798	93.15	1.498
38.40	3.807	96.80	0.973
42.05	3.808	98.99	0.529
45.70	3.808	100.00	0.000
49.35	3.802		

TABLE II

ORDINATES OF THE ZRS–4 MODEL

Station	Ordinates	Station	Ordinates
Inches	*Inches*	*Inches*	*Inches*
0	0	26	3.92
1	0.91	30	3.74
2	1.75	34	3.41
4	2.60	38	2.86
6	3.11	40	2.50
8	3.46	42	2.06
10	3.69	44	1.54
14	3.91	46	0.87
18	3.98	47.4	0.00
22	3.99		

TABLE III

CENTER OF BUOYANCY POSITION AND VOLUME OF MODELS

Model	Length of model	Center of buoyancy per cent length from nose	Volume
	Inches		*Cubic inches*
GZ–3.6	27.4	45.88	860
GZ–4.8	36.5	45.92	1,147
GZ–6.0	45.7	45.88	1,435
GZ–7.2	54.8	45.85	1,720
GZ–5.3	40.3	46.32	1,319
GZ–5.6	42.6	47.30	1,545
GZ–5.8	44.1	46.6	1,490
GZ–6.8	51.7	47.1	1,833
ZRS–4	47.4	45.7	1,605

TABLE IV

AVERAGE STATIC PRESSURE GRADIENTS IN OLD CLOSED-THROAT TUNNEL

Tank pressure (atmospheres)	Static pressure gradients $\left(\frac{\Delta p}{q\Delta d}\right)$		
	Inches from honeycomb		
	25 to 31	31 to 40	40 to 78
1	+0.075	+0.104	−0.014
2.5	−.063	+.088	−.013
5	−.136	+.110	−.018
10	−.225	+.127	−.022
15	----------	+.117	−.022
20	−.325	+.114	−.024

TABLE V

LOCATION OF MODELS IN TUNNELS

OLD CLOSED-THROAT TUNNEL

Model	Distance of nose from honeycomb
	Inches
GZ–3.6	38.79
GZ–4.8	35.13
GZ–5.3	35.13
GZ–5.6	32.70
GZ–5.8	35.13
GZ–6.0	31.44
GZ–6.8	29.05
GZ–7.2	27.84

OPEN-THROAT TUNNEL (NORMAL POSITION)

Model	Distance of nose from entrance cone
	Inches
GZ–4.8	8.8
ZRS–4	4.7

TABLE VI

TESTS

Model	Pitch angles (degrees)	Tank pressures (atmospheres)	Fins	Car
GZ–3.6	0	1, 2½, 5, 10, 15, 20		
Do	0	1, 2½, 5, 10, 20	3.6 brass [5]	Small.
Do	−4–+16	do		
Do	−4–+16	1, 10, 20	3.6 brass	Do.
GZ–4.8	0	1, 2½, 5, 10, 20		
Do	−9–+20	do		
Do	−9–+20	1, 10, 20	4.8 "V"	Do.
Do.[1]	−15–+15	5, 10, 20		
Do.[1]	−15–+15	1, 20	4.8 "V"	
Do.[1]	0	1, 2½, 5, 10, 20		
Do.[1 2]	0	do		
Do.[1 2 3]	0	do		
Do.[1 2 4]	0	do		
GZ–6.0	0	do		
Do	0	do	6.0 "V"	Large.
Do	−9–+20	do		
Do	−9–+20	1, 10, 20	6.0 "V"	
Do	−9–+20	do	do	Do.
GZ–7.2	0	1, 2½, 5, 10, 20		
Do	0	do	7.2 brass	Do.
Do	−4–+16	do		
Do	−4–+16	1, 10, 20	7.2 brass	Do.
GZ–5.3	0	1, 2½, 5, 10, 20		
Do	−4–+16	1, 10, 20		
GZ–5.6	0	1, 2½, 5, 10, 20		
Do	−4–+16	1, 10, 20		
GZ–5.8	0	1, 2½, 5, 10, 20		
Do	−9–+20	do		
Do	−9–+20	1, 10, 20	6.0 "V"	Do.
GZ 6.8	0	1, 2½, 5, 10, 20		
Do	−4–+16	1, 10, 20		
ZRS 4 [1]	0	1, 2½, 5, 10, 20		
Do.[1]	−15–+15	do		
Do.[1]	−15–+15	do	ZRS–4	ZRS–4.

[1] Model tested in open-throat tunnel.
[2] Model tested 8 inches downstream from normal position.
[3] Model tested with highly polished surface.
[4] Model tested with roughened surface.
[5] Fin numbers are the fineness ratio of the model for which the fins were made.

U. S. GOVERNMENT PRINTING OFFICE: 1931

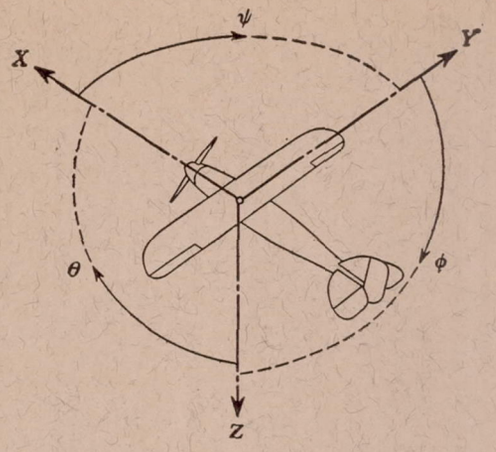

Positive directions of axes and angles (forces and moments) are shown by arrows

Axis		Force (parallel to axis) symbol	Moment about axis			Angle		Velocities	
Designation	Symbol		Designation	Symbol	Positive direction	Designation	Symbol	Linear (component along axis)	Angular
Longitudinal	X	X	rolling	L	$Y \longrightarrow Z$	roll	ϕ	u	p
Lateral	Y	Y	pitching	M	$Z \longrightarrow X$	pitch	θ	v	q
Normal	Z	Z	yawing	N	$X \longrightarrow Y$	yaw	ψ	w	r

Absolute coefficients of moment

$$C_l = \frac{L}{qbS} \qquad C_m = \frac{M}{qcS} \qquad C_n = \frac{N}{qbS}$$

Angle of set of control surface (relative to neutral position), δ. (Indicate surface by proper subscript.)

4. PROPELLER SYMBOLS

D, Diameter.
p, Geometric pitch.
p/D, Pitch ratio.
V', Inflow velocity.
V_s, Slipstream velocity.
T, Thrust, absolute coefficient $C_T = \frac{T}{\rho n^2 D^4}$
Q, Torque, absolute coefficient $C_Q = \frac{Q}{\rho n^2 D^5}$
P, Power, absolute coefficient $C_P = \frac{P}{\rho n^3 D^5}$.
C_s, Speed power coefficient $= \sqrt[5]{\frac{\rho V^5}{P n^2}}$.
η, Efficiency.
n, Revolutions per second, r. p. s.
Φ, Effective helix angle $= \tan^{-1}\left(\frac{V}{2\pi r n}\right)$

5. NUMERICAL RELATIONS

1 hp = 76.04 kg/m/s = 550 lb./ft./sec.
1 kg/m/s = 0.01315 hp
1 mi./hr. = 0.44704 m/s
1 m/s = 2.23693 mi./hr.

1 lb. = 0.4535924277 kg
1 kg = 2.2046224 lb.
1 mi. = 1609.35 m = 5280 ft.
1 m = 3.2808333 ft.